Progress in Nuclear Energy 85 (2015) 297–318

Contents lists available at ScienceDirect

Progress in Nuclear Energy

journal homepage: www.elsevier.com/locate/pnucene

Review

The use of ionising radiation to image nuclear fuel: A review

Helen M. O'D. Parker*, Malcolm J. Joyce

Department of Engineering, Engineering Building, Lancaster University, Lancaster, LA1 4YW, UK

ARTICLE INFO

Article history:
Received 9 September 2014
Received in revised form
27 May 2015
Accepted 5 June 2015
Available online 20 July 2015

Keywords:
Radiation
Imaging
Radiography
Tomography
Nuclear fuel
Special nuclear material

ABSTRACT

Imaging of nuclear fuel using radiation has been carried out for decades for a variety of reasons. Two important reasons are Physical Invertory Verification (PIV) and Quality Assurance (QA). The work covered in this review focuses on the imaging of nuclear fuel using ionising radiation. The fuels investigated are both fresh and spent, composed of assorted materials, and in various physical forms. The radiations used to characterise the nuclear fuel include γ, α, β, muons, neutrons and X-rays. The research covered in this review, spans the past four decades and show how the technology has developed over that time. The advancement of computing technology has greatly helped with the progression of the images that are produced. The field began with 2D images in black and white showing the density profiles of γ rays from within an object, culminating in 2013 when a pebble bed fuel element was reproduced in 3D showing each 0.5 mm UO_2 globule within it. With the ever increasing computing technology available to the industry, this can only mean an increase in the rate of development of imaging technologies like those covered in this review.

1. Introduction

The imaging of items across a diverse range of industrial sectors, using radiation is a widely established technique for Quality Assurance (QA) and verification purposes. Within industry, imaging is used extensively to help carry out tasks such as: flaw detection, failure analysis, assembly analysis and tolerance checks. Imaging can be undertaken using a range of radiations and the form of the results can vary widely from black and white density images to full 3D recreations of whole objects and their internal parts.

Of specific relevance to the nuclear industry, ionising radiation has been utilised for imaging during each stage of the fuel cycle for a number of decades with various purposes [Sawicka et al. (1990); Brenizer (2013)]. For example, currently each Pressurised Water Reactor (PWR) fuel rod manufactured, has a record of the cladding welds to prove that they were fully functional when the fuel rod was assembled [Crossland (2012)]. As well as verification, radiography can be utilised to calculate the enrichments of fuel rods, which can be used for safeguarding purposes.

Imaging of Special Nuclear Material (SNM) can be accomplished by various techniques. The two distinct techniques apparent are *passive* and *active* interrogation. Passive detection is when an object has its intrinsic radioactivity measured. Active interrogation is when an object is subjected to a source of external radiation in order to stimulate a response; this is then measured using a detector. *Passive* and *active* are interchangeable with emission and transmission respectively, throughout this paper. Passive interrogation is mainly used for objects with high activity levels, and active interrogation is generally used for materials which would struggle to be detected passively because they have a lower intrinsic activity.

When carrying out active interrogation there are a number of radiations that can be utilised to bombard the object being assayed. These generally fall into one of the following categories: γ-rays, α particles, X-rays, muons and neutrons. Each stimulates a different response, producing data and images that can be utilised in a number of ways. There is also a wide variety of assay times depending on the source material.

Below is a review of imaging techniques that have been used specifically for nuclear fuel assay since its inception in the 1940's. Following that is a discussion about the current state and a summary of future work that may be beneficial to the industry.

No new data were created during this study.

2. Safeguards

The Nuclear Non-Proliferation Treaty (NNPT) was introduced in 1968, the original aim of which was to stop commercial nuclear material being turned into nuclear weapons, and therefore to

* Corresponding author.
E-mail address: h.parker@lancaster.ac.uk (H.M.O'D. Parker).

http://dx.doi.org/10.1016/j.pnucene.2015.06.006

reduce the amount of nuclear weapons being manufactured worldwide. The original signatories were the USA, the UK, the Soviet Union, France and China. Countries which declined to sign, even though they had demonstrated nuclear prowess were Israel, India, Pakistan, Brazil and Argentina. Since the treaty first began, 189 countries have signed up and North Korea is the only country to have withdrawn their membership [Doyle (2011)].

The nuclear industry within the jurisdiction of the NNPT has to conform to a number of safeguarding responsibilities. These activities minimise the risk of nuclear proliferation in two ways; the first is being able to detect the illicit diversion of SNM from peaceful activities to non-peaceful activities in a timely manner. The second is the possibility that detection may occur, which dissuades potential clandestine operators from trying to carry out proliferation activities. As well as the responsibilities held by the nuclear institutions themselves, the International Atomic Energy Agency (IAEA) are an example of a body who perform Physical Inventory Verification (PIV) tasks to confirm that declared amounts and enrichments of nuclear materials are correct. These data, as well as that provided by the nuclear institutions, are used to provide Continuity of Knowledge (COK). Essentially from mining to spent fuel storage, all SNM should have a documented COK trail associated with it.

Nuclear institutions have to counter any credible diversion strategy for SNM. Diversion strategies generally fall into two categories: the removal of nuclear material that is subject to safeguards and the misuse of safeguarded facilities [Shea and Chitumbo (1993)]. This review will only be concerned with the former. The IAEA uses three definitions for the difference between declared amounts of nuclear fuel and the material present, *gross* defect, *partial* defect and *bias* defect. A gross defect is one in which most or all of the material declared is missing from the object. A partial defect is one in which some fraction of the declared material is missing from the object and a bias defect is one in which only a small fraction of the declared material is missing [IAEA (2002)]. Non-Destructive Assay (NDA) has been a staple method in safeguarding, both passively and actively, using various radiation types and employing different methods by which to deduce information about the assayed material [Hsue et al. (1978); Behrens et al. (1979); Runkle et al. (2012); Levai (1982)]. Safeguarding work pertaining to NDA image production are reviewed below.

2.1. Partial defect detection

The largest collection of work into safeguarding technologies works towards the detection of a rod being diverted from an assembly of spent fuel. This scenario is seen to be of particular interest as the spent fuel would contain a potentially significant amount of plutonium which could be used for a variety of clandestine operations. One of the methods by which to detect a partial defect is to carry out a passive assay of the γ radiation being emitted from the spent fuel. This technique is described in Lee et al. (1997); Jacobsson et al. (2000); Jacobsson (2000); Svard et al. (2006); Lundqvist et al. (2007); Jacobsson Svaerd et al. (2008).

Both Lee et al. (1997) and Jacobsson et al. (2000) use an Algebraic Reconstruction Technique (ART) in order to analyse the data gained during γ assay [Gordon (1974)]. The results of their tomography of a spent fuel assembly were presented in graphical form; this allows the reader to see clearly that a rod is missing or replaced. In Lee et al. (1997), the graphs produced are two dimensional and the reader may only observe one row of the fuel bundle at a time, whereas Jacobsson et al. (2000) has managed to assemble all of the cross section graphs from one plane together to make a three dimensional graph which can more easily show the diverted rod.

Svard et al. (2006) and Lundqvist et al. (2007) are able to show a well resolved image of a reconstructed assembly.

Svard et al. (2006), compares three γ tomogram techniques for identifying partial defects in spent fuel. These are namely; Pool-side tomography, a laboratory set-up and in-pool tomography. The pool-side tomography is carried out through the spent fuel cooling pond wall. The fuel bundle used is an 8×8 Boiling Water Reactor (BWR) type that had been cooled for 8 years. 3240 detector positions are recorded over the whole assembly. The detectors used in this set-up do not produce an image of the fuel element but a graph is produced which shows the amount of activity at each position within the fuel assembly. It can be seen that with the correct γ spectrum, a missing fuel rod can clearly be identified. In the laboratory experiments mock ups of a fuel assembly are used. These are recreated by filling titanium tubes with granulated copper activated with ^{137}Cs. The aim with this test is to be able to identify a swapped rod and a missing rod. 2072 detector positions are recorded with the time in each position equaling 10 s. Similar to the pool-side measurements, the lab tests also resulted in statistical graphs of how similar each rod was to each other. It can be seen from these graphs that the swapped rod is easier to identify than the missing rod. However, statistically both rod changes are detectable. The mock assembly and tomogram produced can be seen in Fig. 1.

The *in-pool* measurements were carried out at Swedish Nuclear Power Plant Forsmark 2. The equipment used is highly specialist and is described in greater detail in Jansson et al. (2006). The fuel assembly used was a BWR of the *SVEA-96S* variety and had only been cooled for 1 year. With the cooling time being so short, it was decided that the most suitable isotope for tomographic measurements was ^{140}Ba. The research utilised 10,200 detector positions, but the article does not say how long this took overall or per detector position. The bundle set up and the tomogram produced are shown in Fig. 2. This test did not include the removal or swapping of any of the pins, presumably due to the difficulties involved with such a task. The image does however show a very clear likeness to the assembly. In comparison to the laboratory measurements provided above, this image has been made clearer by subtracting the background noise and therefore minimising the impact of contaminant γ rays.

Similarly, Lundqvist et al. (2007) simulated an assembly and the associated tomography (Fig. 3) to show very similar results to Svard et al. (2006). Then another tomograph is produced from measured data for comparison. However, this measured data does not contain a partial defect. Instead it is a spent fuel assembly that had recently been removed from service (Fig. 4). It appears on both the simulated tomograph and the tomograph that uses measured data, that

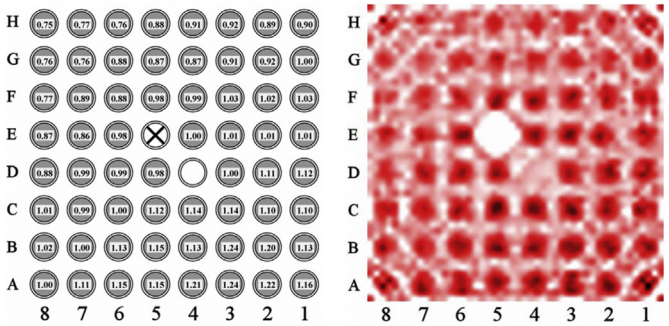

Fig. 1. Laboratory mock up of a BWR spent fuel assembly on the left showing the swapped rod marked by an 'X' and the missing rod shown empty. The right image is the corresponding γ tomogram. Image reconstruction using only γ attenuation information was used here [Svard et al. (2006)].

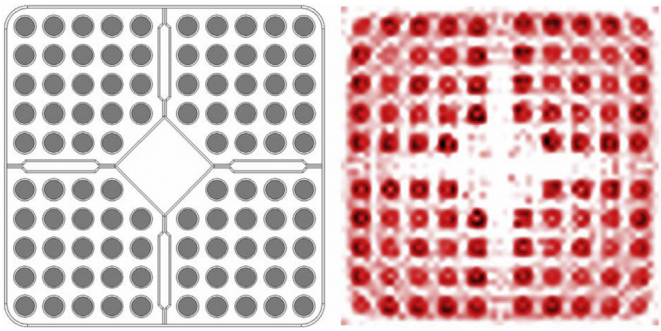

Fig. 2. Schematic of a spent BWR SVEA-96S bundle assembly on the left and the γ tomogram produced on the right. Rod-activity reconstruction is used here, which utilises prior knowledge of the geometry of the bundle. This allows for more accurate reconstructions [Svard et al. (2006)].

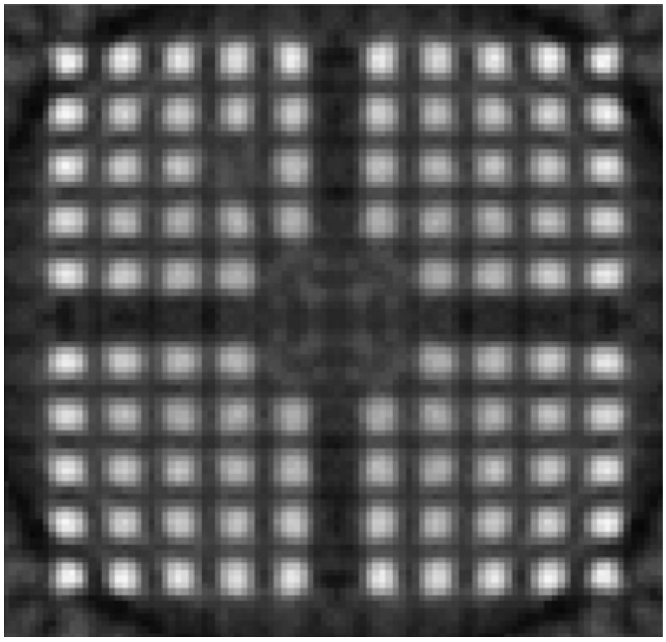

Fig. 3. A γ tomograph reconstructed from simulated data showing a missing rod from a spent fuel assembly (top left) [Lundqvist et al. (2007)].

the activity levels of the rods reduce with an increased proximity to the centre of the assembly. This is due to the use of emitted γ as the measured variable. The γ rays from the centre of the assembly are attenuated and scattered before they reach the edge where they may be detected. The γ rays being emitted from the edge of the assembly have a much clearer pathway and therefore have a better chance of interaction with the detection equipment.

Exploiting neutrons emitted offers the potential to reduce the effects of attenuation and scattering within the fuel bundle as they are more penetrating through SNM. Hausladen (2013) utilises emitted fast neutrons to produce an image of an assembly of fresh Mixed Oxide (MOX) fuel (Fig. 5). The mock-up assembly used contained 31 rodlets of fresh MOX fuel and one rodlet filled with depleted uranium. The MOX rodlets contain 3.66 g of ^{240}Pu which produces roughly 3700 neutrons s^{-1} from spontaneous fission. The work was carried out as a test run to verify that the collimation setup would work equally well for spent fuel. If the system were to be used on spent fuel, the detection equipment would need to be modified by making it less susceptible to γ radiation. Changing the detector material from a liquid scintillator could have an effect on

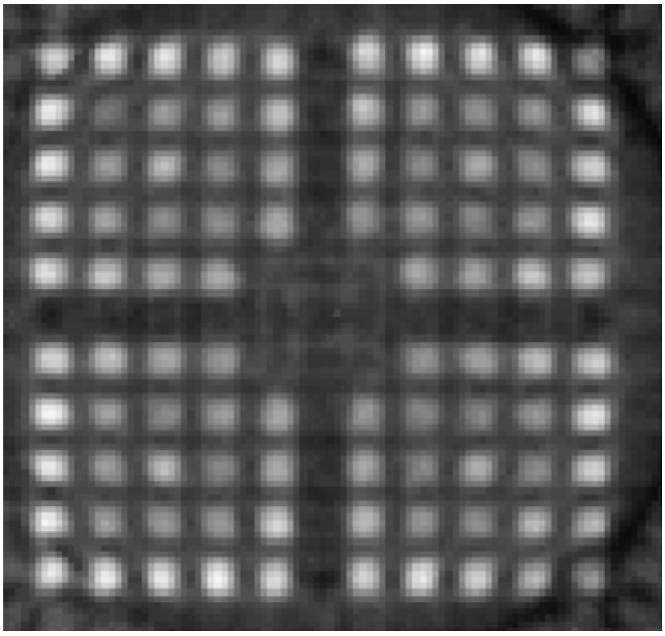

Fig. 4. A γ tomograph reconstructed from measured data, showing all rods in place in a spent fuel assembly [Lundqvist et al. (2007)].

measurement efficiency and also scattering, which could affect the resolution of the image produced.

As well as passively assaying fuel bundles for diversion defects, a radiation source can be used to stimulate a response from the fuel bundle, that can then be measured. Steinbock (1990, 1991), describe a feasibility study for a portable tomography kit that could be used during PIV. Both focus on using a variety of radiation sources to produce tomograms of phantoms of spent fuel for safeguarding purposes. The images produced do not show a partial defect scenario specifically but the method would remain the same for PIV tasks. The use of X-rays, betatron and thermal neutron sources are all described within both papers. The abstracts both refer to imaging fresh fuel as well as spent fuel, but only spent fuel is eluded to within the text of each paper. The setup used within the experiments utilises two slit collimators in order to produce a fan beam which is detected by a line scan camera. Firstly an X-ray sinogram and tomogram have been produced of a BGS4 pin, within which the fuel had melted during an overpower test. The tomograph shows the three concentric tubes of zircalloy, molybdenum and niobium

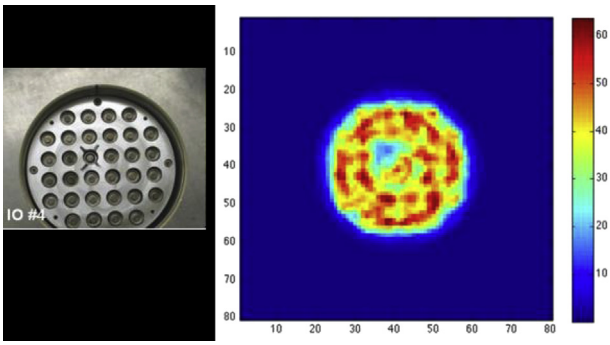

Fig. 5. Assayed assembly (left) showing the DU pin marked by an 'X'. The emitted fast neutron tomograph (right), identifying the position of the DU pin. Deconvoluted using maximum likelihood expectation maximization (MLEM) [Hausladen (2013)].

and the fuel distribution with some cladding steel inside a pocket. The image can be seen in Fig. 6.

Following the X-ray images are neutron images of both a 6-pin and a 19-pin phantom assembly. The pins were made of steel tubes filled with boron and epoxy resin. The neutron beam energy was set to 0.025 eV (thermal neutrons). Steinbock attributes the noisiness of the 6 pin image to the fact that neutron transmission was reduced when the pins were aligned, however the 19 pin assembly is not discussed in this regard. The images for both the 6 and the 19 pin assemblies can be seen in Fig. 7 and Fig. 8 respectively.

Finally the betatron source was used to create images of hot cells using phantoms. The betatron source was an 18 MV source. The betatron intensity was manually controlled and so the sinograms obtained contained variations. The phantoms were recreated using 21 pins in an assembly with one of the set-ups being a split between lead and lead/epoxy resin and another including a mixture of lead and aluminium. There was also a phantom made from two tungsten prisms with ten tantalum sheets spanning the gap between. As can be seen in Fig. 9, it is difficult to differentiate between both the lead and aluminium in Fig. 9(a) and lead and lead/epoxy in Fig. 9(b). Similarly, the tantalum sheets in Fig. 9(c) can be identified only when it is known that they are there *a priori*. In order to be able to gain any confidence in differentiating between these materials, the method would need to be improved, or the results would need to be analysed computationally.

At the time this paper was published the methods described could image down to a resolution of 0.3 mm, and screens had been developed to go down to 0.1 mm in the future. The author also described a method, using 0.05 mm thick scintillators, which would be able to achieve a resolution of 0.1 mm if they were able to increase scanning time ten-fold.

Similarly to their previous work in 1997, Lee et al. (2001) uses tomography again to examine spent fuel bundles to reduce the chance of diversion, however, this time an active interrogation method is used. Neutrons between 0.1 eV and 1 keV were used to stimulate fission to identify fissile material. The interrogating neutrons induce fission in fissile materials, but not greatly in fertile materials. These fission neutrons are then detected in an array of ^{238}U threshold detectors. The results of the tomography are presented as graphs of the cell density. Fuel rods that are missing can be seen on the corresponding graphs. This remains true even if the material from the 'diverted' rod is moved into the surrounding rods, i.e. if the total fissile mass remains constant.

2.2. Detecting nuclear fuel in storage containers

The detection of nuclear materials inside containers has been researched in detail, however, this review only covers the imaging of nuclear fuel. Jonkmans et al. (2010, 2013) look into the feasibility of using muons to produce tomograms of spent fuel inside containers. Simulations are used to create images using Point of Closest Approach (POCA), Maximum Likelihood Expected Maximisation (MLEM)[Bruyant (2002)], and Scattering Density Estimation (SDE) reconstructions. The images produced show the spent fuel in a variety of containers from steel drums to Dry Storage Containers (DSC) (Figs. 10–12 respectively).

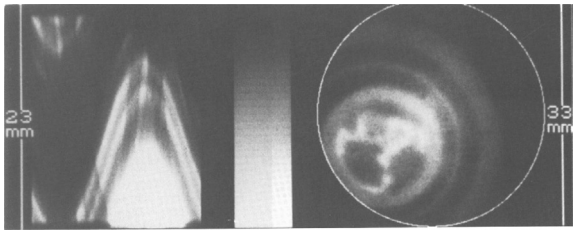

Fig. 6. Sinogram (left) and tomogram (right) of X-ray interrogation of a BGS4 pin [Steinbock (1991)].

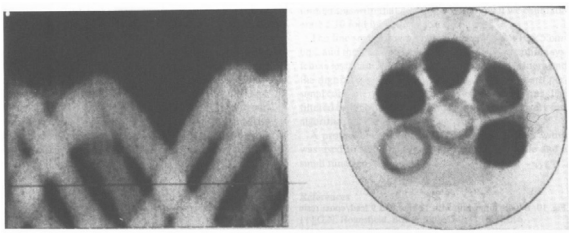

Fig. 7. Sinogram and tomogram showing a set of 6 phantom pins interrogated by a 0.025 eV neutron beam [Steinbock (1991)].

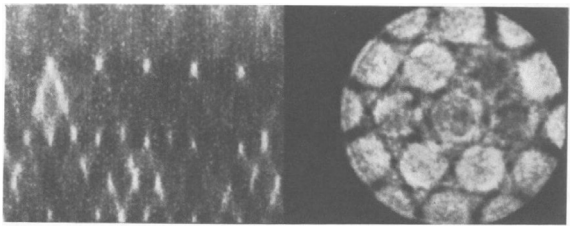

Fig. 8. Sinogram and tomogram showing a set of 19 phantom pins interrogated by a 0.025 eV neutron beam [Steinbock (1991)].

As there are only certain facilities licensed to receive and store spent nuclear fuel, spent fuel must be transported either nationally or internationally. Containers are necessary for activities such as transport; being able to non-destructively ascertain SNM levels of spent fuel within a container allows for a higher level of COK and therefore safeguarding.

3. Quality assurance

During fabrication, use, and disposal of nuclear fuel, there must be a very high level of QA to ensure the safety of people and assets. NDA is used within the nuclear industry to ensure compliance with strict QA rules [Mistry et al. (1996)]. QA can cover an abundance of properties that the fuel must possess in order to be classed as suitable for use in Nuclear Power Plants (NPPs). Parameters such as geometry, enrichment, agglomerates, rod loading, and failure modes will be covered here. There are obviously different parameters to be verified when the fuel is fresh, during irradiation, spent, and during storage (particularly long term storage). The geometry of fuel elements, from their size, to their intactness, has been the subject of numerous works using radiation and imaging, for both fresh and spent fuel [Levai (1982); Domanus (1984); Dande et al. (1991); Kumar et al. (2000); Kuzelev and Yumashev (2001)].

A general overview of Non-Destructive Testing (NDT) methods used can be found in Gozani (1981). With regards to nuclear fuel the work does not cover imaging but it does cover all of the major types of non-destructive assay of nuclear material. There is a whole chapter on the γ scanning of fuel rods. Bearing in mind that this technology is still used to quantify fresh nuclear fuel today it shows how little the field has progressed in over 30 years. Research has continued into new techniques and methods [Ghosh et al. (1983a); Panakkal (2013)] but the industry has yet to take them up in earnest.

The following section is split broadly into fresh fuel QA, and spent fuel QA.

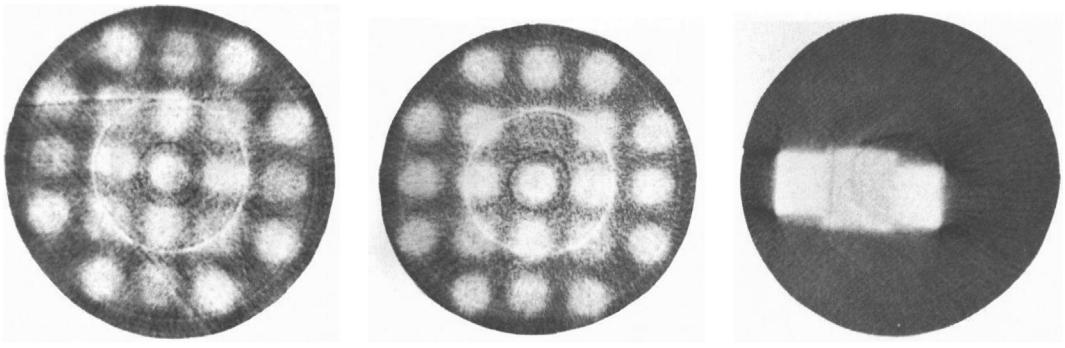

Fig. 9. 18 MV betatron images of (a) 20 lead pins and one aluminium, (b) 12 lead pins and 9 lead/epoxy resin pins and (c) a tungsten tantalum phantom [Steinbock (1991)].

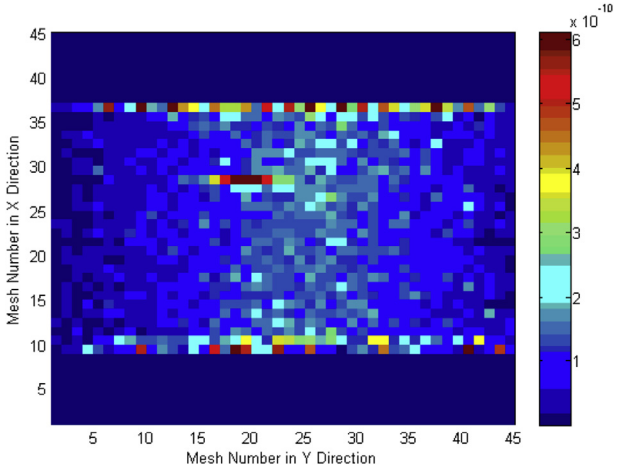

Fig. 10. A simulated result of a single UO_2 fuel pin lay on its side tomographed using muons and the MLEM reconstruction technique [Jonkmans et al. (2013)].

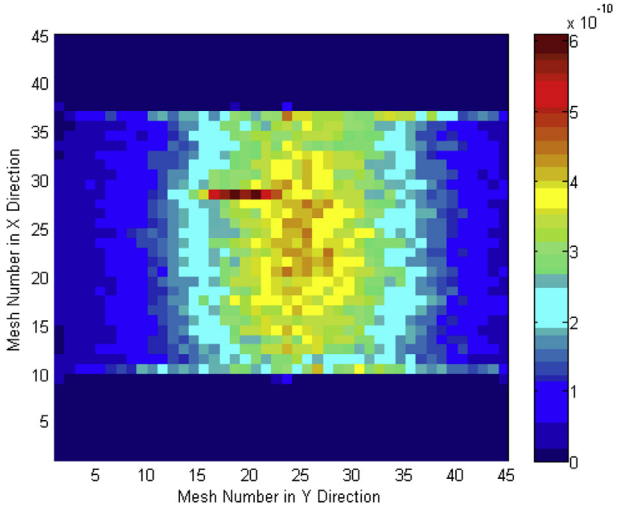

Fig. 11. A simulation of a single UO_2 fuel pin lay on its side tomographed using muons and the SDE reconstruction technique [Jonkmans et al. (2013)].

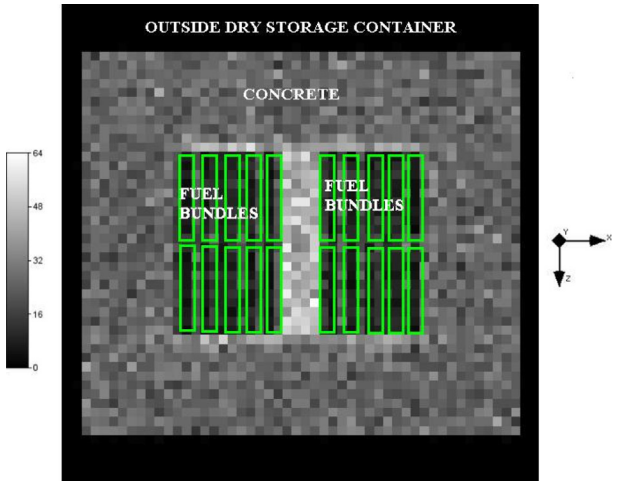

Fig. 12. The results of muon tomography on simulated fuel bundles within a Dry Storage Container (DSC) [Jonkmans et al. (2013)].

3.1. Fresh fuel QA

Fresh nuclear fuel is manufactured in stages and each stage has the potential for the introduction of defects. In brief, fuel fabrication of the most abundant types of fuel (assemblies of rods of nuclear fuel pellets), can be split into three areas, powder production, pelletisation and sintering, and rod assembly. For the purposes of this review, only items at, or after the pelletisation stage will be taken into account, as this is when the material becomes nuclear fuel. During pelletisation and sintering, the powder mixture is pressed into the required shape and then sintered. These ceramic pellets are then passed through to the rod assembly area where they are stacked into zirconium alloy rods. These rods are then filled with helium and welded to completely seal the contents. The welded rods are then pulled into assemblies of varying geometries depending on the type of fuel.

At pelletisation and sintering the main defects considered are agglomerates, inhomogeneity and chips or cracks within the pellets. At rod assembly there is the possibility of loading the wrong type of pellets, in terms of both compound, enrichment and shape. There are also defects to be considered in the ancillary equipment and rod itself.

3.1.1. Internal and external geometry

Firstly the problem of chips, cracks and pitting is reviewed. Lekeaka-Takunju et al. (2009, 2010, 2011); Kim (2010) all simulate the use of X-ray tomography in order to be able to see geometrical defects in the periphery of fuel pellets. The point here being that currently only a sample of fabricated pellets are tested for these defects because the testing is destructive. When only testing

samples, it is impossible to guarantee 100% of pellets are within specification. If NDT imaging or similar was used on the fabricated pellets then 100% of the pellets could be verified. This would require the test facility to be in-line with production and therefore the number of projections (images produced from a single location and angle) and the length of each projection needs to remain small. A novel technique is suggested [Lekeaka-Takunju et al. (2010)] to increase image resolution with fewer projections than previously necessary.

In order to maintain good image quality with fewer projections a *convex interpolation* was used with the mathematical Radon transform [Svalbe and van der Spek (2001)]. The convex interpolation method allows the Radon transform to be filled between the obtained projections. It can be seen in Fig. 13 that the binary threshold versions of the original and reconstructed image are similar and that the crack can be seen clearly in the reconstructed image despite fewer projections. This technique could be deployed with other tomography techniques and allow for a reduction of projections on the items being imaged.

Agglomerates in fuel (particularly MOX fuel) can cause hotspots during the irradiation process. As plutonium agglomerate production is statistical in nature, it can be argued that it is highly likely that they will appear in the periphery of the pellet and be detectable by gamma autoradiography [Ghosh et al. (1984)]. Also, some isotopes of plutonium are α emitters so plutonium agglomerates can be detected by α autoradiography. An agglomerate in the region of 125–2000 μm can be seen in a UO_2–4% PuO_2 MOX pellet in Fig. 14. Methods of autoradiography are cheaper and more straightforward than transmission neutron radiography or tomography; this would be a factor if these methods were to be considered for use in industry.

Autoradiographs of fuel and its intrinsic agglomerates or enrichment differences can be viewed by operators who could then make a decision about whether what is seen is acceptable.

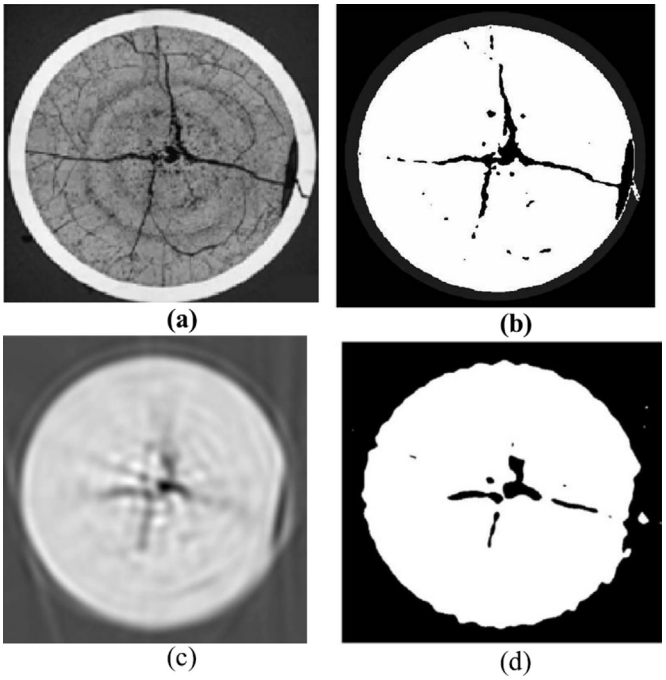

Fig. 13. Crack detection using X-ray tomography with only 30 projections. (a) The optical image. (b) Binary threshold image of (a). (c) Reconstruction of (a) with convex interpolation. (d) Binary threshold image of (c). Reconstructions were carried out using a Radon transform [Lekeaka-Takunju et al. (2010)].

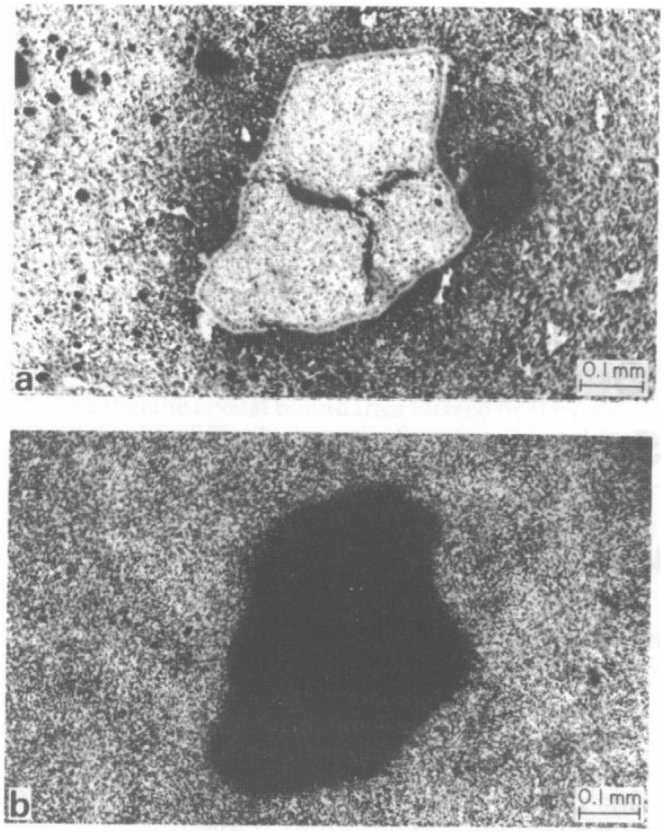

Fig. 14. A PuO_2 agglomerate seen in an MOX pellet (a) photomicrograph image and (b) an alpha autoradiograph image [Ghosh et al. (1984)].

However, this method leaves room for discrepancies from human error. This is particularly true for black and white images, for which the human eye may struggle to separate image densities that are similar. One way to combat this issue is to introduce a colour scale by which the density of the image can be identified much more clearly. This method can be seen in Figs. 15 and 16 [Panakkal and Mukherjee. (2008)].

The original image is a Gamma Auto Radiograph (GAR), produced by keeping the fuel rod in contact with X-ray films in a cassette. These images were then digitised and a colour segmentation technique was applied. This allows contours of optical density levels to be seen clearly as shown in Fig. 16. The methods used to produce the black and white images were routine by 2008 but the digitising, and therefore colouring of the images is a newer aspect. There is no detail describing the use or need of the presented technology, but it is possible to infer that it may be easier for

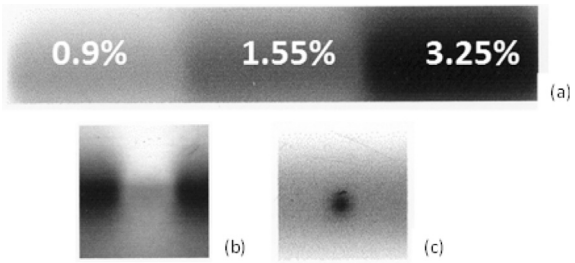

Fig. 15. Original γ autoradiographs of (a) various enrichments of PuO_2 in pellets, (b) a medium enrichment pellet in a high enrichment rod and (c) a PuO_2 agglomerate in the outer layer of the pellet [Panakkal and Mukherjee. (2008)].

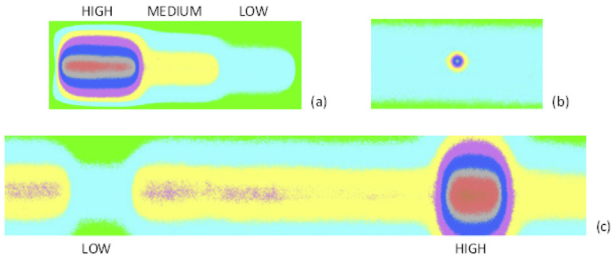

Fig. 16. Digitised γ autoradiographs of (a) various enrichments of PuO_2 pellets (b) a PuO_2 agglomerate in the outer layer of a fuel pellet and (c) pellets of mixed enrichment in a pin [Panakkal and Mukherjee. (2008)].

a human to differentiate between the different areas. Although it could be argued that using a computerised optical densitometer would remove all risk of human error.

When trying to obtain an assessment of agglomerate deposition in a fuel pellet, gamma rays sometimes do not penetrate far enough through the item. For instance, agglomerates within fuel can be seen physically with gamma autoradiographs only if they are near to the surface, but as shown in Fig. 17, neutron interrogation can be used to identify agglomerates through the whole cross section of a pellet [Ghosh et al. (1983b, 1984); Panakkal et al. (1992); Ghosh et al. (1997)].

So far only cylindrical fuel pellets have been considered, however, other types of fuel also have agglomerate-type particles. Spherical fuel for instance, has coated particles of UO_2 dispersed within a graphite matrix. Important parameters of this type of fuel can be imaged using radiation: the thickness of the coating on each individual fuel particle, the *fuel free zone* of the spherical element to ensure it is in fact fuel free, and the homogeneity of the UO_2 dispersal throughout the pebble [Tisseur et al. (2007)].

One of the more comprehensive images produced, showing a fresh pebble fuel element was obtained using neutron imaging [Lehmann et al. (2003)]. The image shows a full fuel pebble with each individual fuel particle evident throughout (Fig. 18). Thermal and cold neutrons were used to investigate various types of fuel and some of the work is similar to work in other papers showing cracks

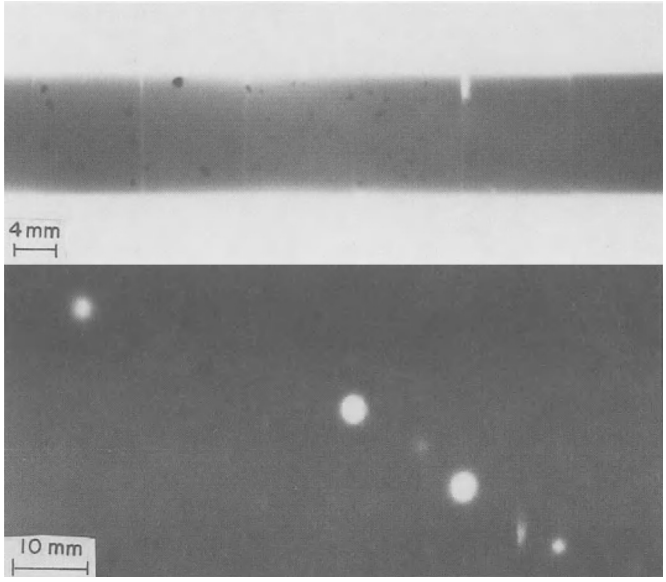

Fig. 17. PuO_2 Agglomerates shown in (top) neutron radiograph and (bottom) γ autoradiograph [Panakkal et al. (1992)].

in spent fuel, hydride lenses in the outer cladding layer of a tube and hydrogen accumulation in the cladding material. The image that seems to push the boundaries of the work is a full 3D reconstruction of a fuel pebble.

A thermal neutron source with a flux of 8.1 x 10^6 n cm^{-2} s^{-1} and a collimation ratio of L/D 350 was used to take 300 sequential projections whilst the sample was rotated by 180°. The nominal spatial resolution was obtained by using a 97 mm field of view. The images were normalised and slices of the pebble perpendicular to the rotation axis were reconstructed by filtered back-projection. The slices were stacked to create a 3D image seen in Fig. 18, as a threshold was introduced to determine whether the neutron attenuation coefficient related to graphite or fissile material.

Similar to the images produced by Hausladen (2013) this image shows specific items within an object. However Lehmann has managed to stack the many 2D images to create a 3D representation. The ability to show a cut-away of the coating and graphite matrix sets this image apart in the field of imaging nuclear fuel. Again, comparing this image against the ones produced by Hausladen, this shows Low Enriched Uranium (LEU) fuel as opposed to MOX fuel, so the images would be physically easier to obtain (fewer health and safety risks). However, they would be harder to create images of, due to the requirement of an interrogating neutron source and the potential issues surrounding collimation and geometry.

Measurement of the coatings of TRISO (LEU) particles has been carried out successfully with X-ray radiography [Kim et al. (2006, 2008); Yang et al. (2013b)]. However, Phase Contrast Imaging (PCI) was used as opposed to ordinary X-ray radiography, as conventional X-ray radiography cannot discern between materials of similar thickness and densities. PCI can be applied to detect phase shift of X-rays at boundaries between two materials that have different refractive indices. As shown in Fig. 19, the PCI X-ray image can then be post processed to show and measure the thicknesses between each layer. The technique uses the Sobel operator to find boundaries and identify the co-ordinates of the *peaks* where boundaries occur [Vairalkar and Nimbhorkar (2012)]. Then the distances between these co-ordinates can be measured.

The *fuel free zone* of pebble type fuel is currently tested destructively, in a batch of 20,540 spherical fuel elements, 99% were deemed to meet the criteria for the fuel free zone. This means that over 200 did not pass. When it is considered that around 27,000 pebbles were loaded into a reactor in China, it can be seen that the rate of failed pebbles could have an effect on the safe running of the reactor [Yang et al. (2013a)]. Again X-ray radiography can be utilised to identify fuel particles in the *fuel free zone* and to remove the risk of human error, the images can be automatically processed as shown in Fig. 20 [Yang et al. (2014)].

As well as agglomerates and fuel particles, there are other aspects of the internals of fuel elements that can be investigated with radiation [Lee et al. (2000)]. Neutrons can be used to discern a solid pellet from an annular one. In Panakkal et al. (1992) neutrons from the APSARA swimming pool type reactor were transmitted through solid and annular pellets. The neutrons were detected directly on gadolinium screens along with Agfa Structurix D2 film. The image produced (Fig. 21) clearly shows the distinction between the two types of pellet.

More recently work has been carried out with neutrons [Tremsin et al. (2013)] to obtain images using more modern technology at Los Alamos. The work utilised a new Micro Channel Plate detector, produced by Nova Scientific which is doped with ^{10}B and Gd. It converts neutrons into electrons at the nearest pore or microchannel. Imaging was carried out with two different exciting neutron energies; cold neutrons and thermal neutrons. Three pellet assemblies were produced each with different aspects that were to

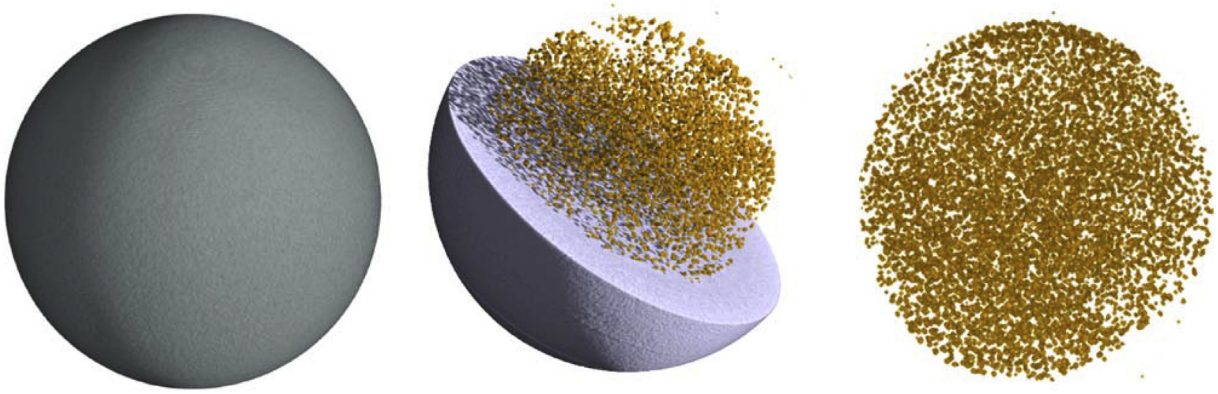

Fig. 18. Sphere type fuel element from the HTR program investigated with neutron tomography. Left: the outer graphite sphere, middle: partly separated particles, right: the 8500 LEU particles. Reconstructions were carried out by using FBP [Lehmann et al. (2003)].

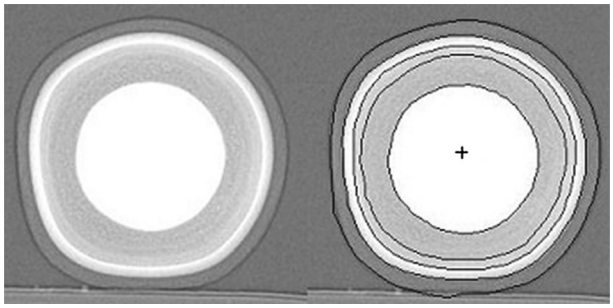

Fig. 19. A PCI X-ray image of a 0.92 mm fuel particle (left). The Sobel operator applied to the original image in order to identify boundaries between each coating layer (right) [Kim et al. (2008)].

be investigated during the testing. The first pellet assembly had varying densities, the second and third had tungsten inclusions and the third also had PMMA (plastic) included which burnt off during the sintering process to leave voids within the pellets. The first images were produced by summing the images around the ^{238}U resonance energies (6.41–6.9 eV, 20.51–21.28 eV and 36.22–37.67 eV). These images (Fig. 22) took several hours to obtain to ensure that enough detected neutrons were available to show the maps of various materials with sub millimetre spatial resolution.

Following the ^{238}U resonance energy images, analysis of the tungsten absorption energy images allowed the images in Fig. 23 to be produced. Thermal neutrons were then used to excite the fuel assemblies. The difference here is that the images took only minutes to be produced, due to the higher detection efficiency for thermal energies.

The images in Fig. 24 show the difference in density of the material more clearly than the previous images and even show the Kapton tape wrapped around the top of each of the assemblies. The thermal resonance images are generally seen to be of better overall quality for the following two reasons: firstly, the resonance energy range used for isotope mapping is much narrower than the thermal and cold neutron spectrum. Secondly, for the setup used in this experiment the detection efficiency for thermal neutron transmission is much higher at around the 40% level. Also contributing to these factors is the high level of divergence of epithermal neutron beams, which is more difficult to collimate in comparison to thermal neutrons.

3.1.2. Validation of new fuels

Imaging of nuclear fuels can be used as a way of validating new types of fuel, whilst still at the experimental phase. This will become more and more important as the nuclear industry tries to use higher burnups and temperatures at reactors, and also as new fuel types become viable [Brown et al. (2014)].

[Baghra et al. (2013)] makes use of; amongst other things; alpha autoradiography to compare a new *impregnated agglomerate pelletisation* (IAP) process to *coated agglomerate pelletisation* (CAP) and the already established *powder pellet process* (POP) for (Th–3.75U) O_2 + X nuclear fuel. The radiography was used to ascertain the distribution of the uranium matrix. A CR-39 film was prepared for radiography (including applying a layer of aluminium Mylar to limit alphas from thorium) and then the pellet was radiographed for 4 h. Following irradiation, the film was chemically and digitally processed to produce a (Uα) track density profile.

From the images produced; in the right hand column of Fig. 25; it is clear that the CAP process produced a less uniform Uα than the IAP and POP processes. Once the images had been processed using image processing software the (Uα) track density profiles were obtained (left hand column). This confirms the non-uniformity of the CAP pellet in comparison to the other two pellets. This technology is useful for quantising something that is qualitative to the human eye. The outcome is very similar to the work described in Section 3.1.1 by Panakkal and Mukherjee. (2008), however rather than colouring in the black and white image, a graph is produced which can be analysed. If these techniques were to be utilised in a QA environment, it would depend upon the requirements of the system as to whether a graphical output or colour image were best for the task at hand.

Likewise, the homogeneity of a possible new fuel, containing PuO_2 dispersed throughout UO_2 has been investigated by use of X-ray radiography and micro computed tomography [Devlin et al. (2009)]. It is hoped that the new fuel would allow for easy separation of actinides and fission products which would largely allow for easier recycling of spent fuel. For the study, surrogates of PuO_2 and UO_2 are used along with a *Xradia* (Concord, CA, USA), and scintillation detectors with a Charge Coupled Device (CCD) camera. The image clearly shows the PuO_2 surrogate particles equally dispersed throughout the UO_2 surrogate (Fig. 26).

Micro X-ray tomography has been undertaken [Lechelle et al. (2004)] to validate a numerical model which describes the behaviour of sintered MOX fuel. The model would reduce the number of laboratory tests if it was validated for use in the industry and as such, it is compared against measured data in the paper. Fig. 27 shows one of the 3D tomograms produced of a UO_2 grain. As can

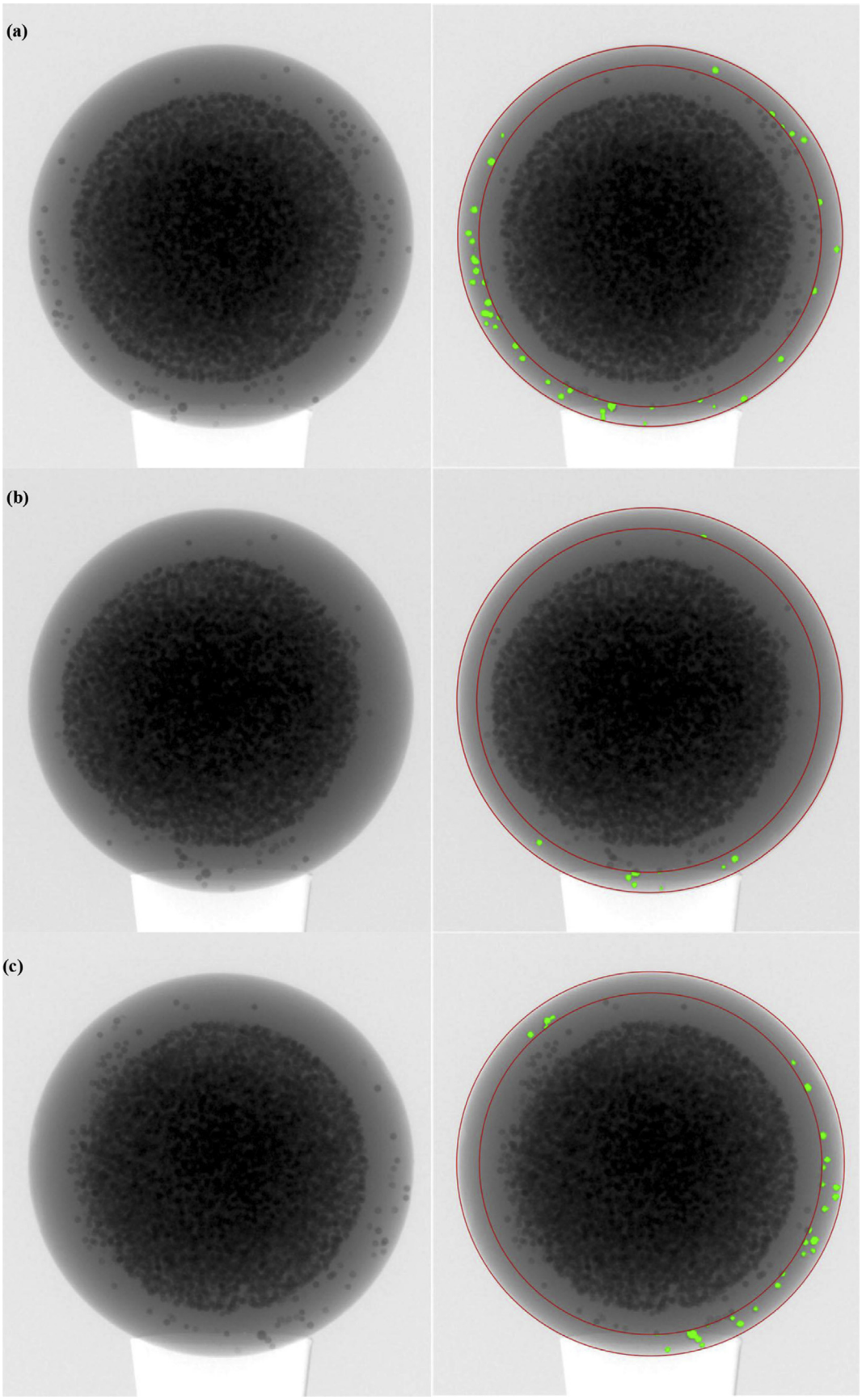

Fig. 20. X-ray radiographs of TRISO (LEU) pebble; the original image and the results of using the automatic detection system at (a) 48° , (b) 96° and (c) 144° [Yang et al. (2014)].

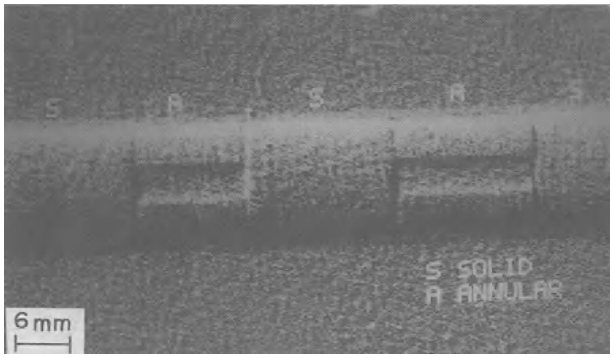

Fig. 21. Neutron radiograph of solid and annular MOX fuel pellets [Panakkal et al. (1992)].

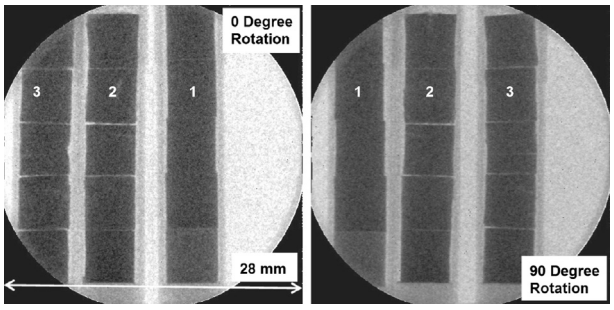

Fig. 22. Images produced from summing the images created at ^{238}U resonance energies. Images are normalised by the open beam images acquired for the same range of energies [Tremsin et al. (2013)].

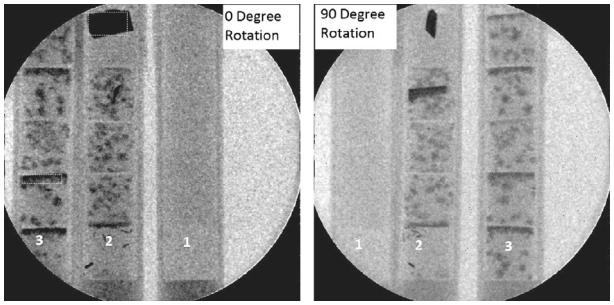

Fig. 23. The addition of images around the absorption for tungsten showing tungsten inclusions, particularly the wedge at the top of assembly 2 [Tremsin et al. (2013)].

be seen on the figure, the resolution seen here is around 40 μm, many orders of magnitude smaller than most other images discussed in this review. This is possible with the use of a FReLoN CCD camera coupled with an optical microscope. This technology shows promise for imaging sub millimetre artifacts in SNM.

3.2. Spent fuel QA

The Quality Assurance of spent fuel rods comes in various forms. Failed rods and assemblies are problematic for NPPs and any information that can be gleaned from a failed rod may be valuable to the nuclear industry. Post Irradiation Examination (PIE) using radiography has been carried out on nuclear fuel extensively, for both intact and failed rods [Richards et al. (1982); Davies et al. (1986); Bakker et al. (1987); Kosarev et al. (1987); Tsupko-Sitnikov (1991); Katsuyama et al. (2010); Ishimi et al. (2012)].

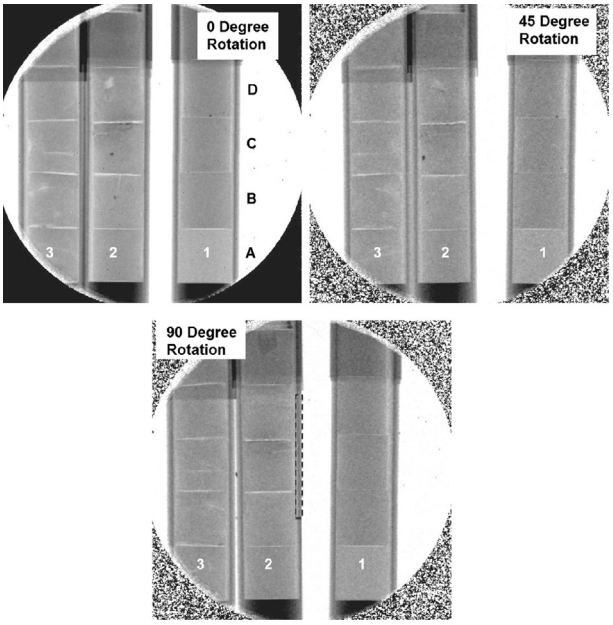

Fig. 24. Assemblies at three angles of rotation showing transmission images using thermal neutrons [Tremsin et al. (2013)].

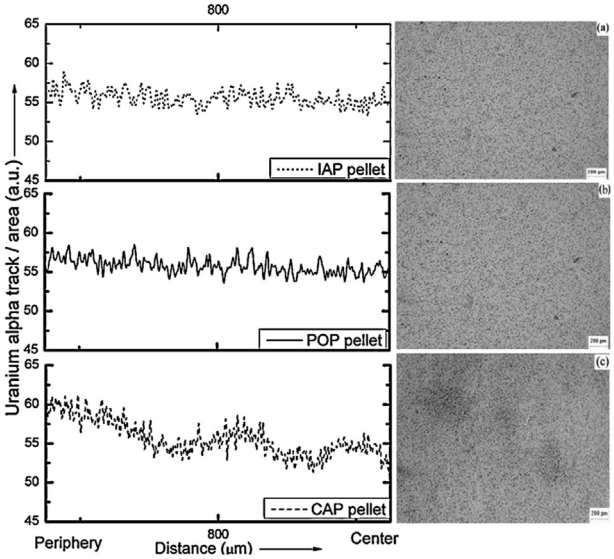

Fig. 25. (Th-3.75% U) O_2 + X pellets Uranium alpha (Uα) track density profiles for (a) Impregnated Agglomerate Pelletisation (IAP), (b) Powder Pellet Process (POP) and (c) Coated Agglomerate Pelletisation (CAP) process [Baghra et al. (2013)].

NDT of spent fuel greatly reduces the cost of examination in comparison to destructive testing, as there is much less need for manipulation of the rod in expensive hot cells, and in a lot of cases the rod can remain in tact, thus containing fission products and radioactive isotopes.

3.2.1. Cladding investigations

Clad integrity is important to the running of NPPs as failures release radioactive isotopes into the primary water circuit, thus reducing working times in certain areas of plant. Therefore, cladding failures need to be picked up urgently. It is in the primary water circuit that detectors identify fission products and alert NPP's operators to a cladding failure problem. Once a failure has been

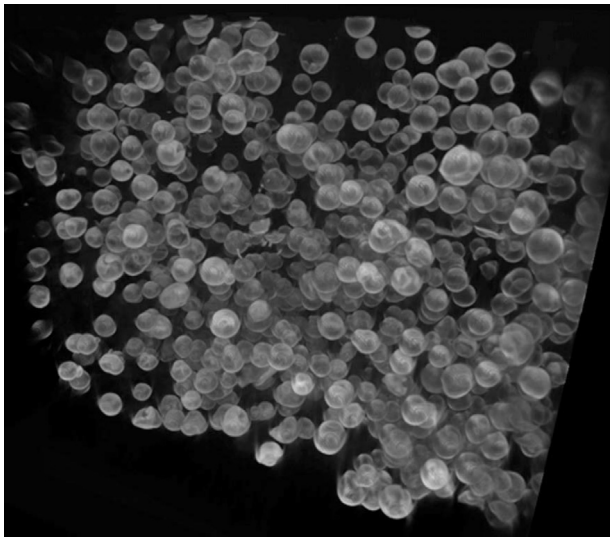

Fig. 26. Micro X-ray computed tomograph of surrogate of PuO_2 dispersed in UO_2. FOV is roughly 1 cm [Devlin et al. (2009)].

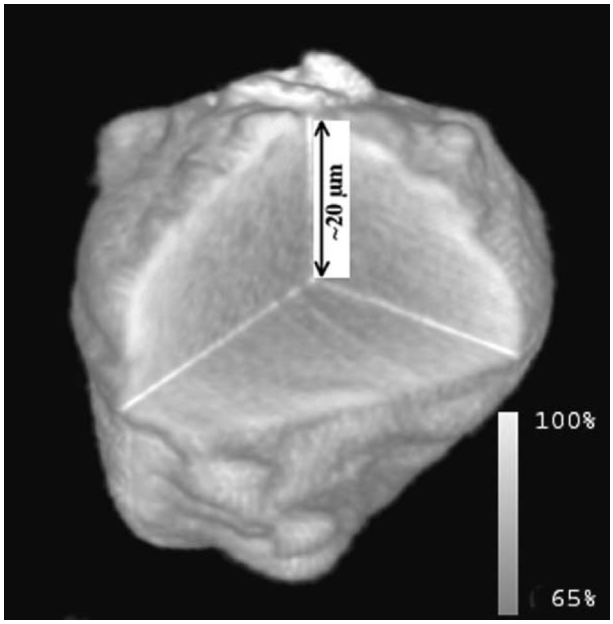

Fig. 27. Micro X-ray computed tomograph of UO_2 grain, showing density across the grain [Lechelle et al. (2004)].

detected, the specific rod or rods need to be identified. One method of identifying a leaking rod is to compare the fission product distribution in the suspected failed rods [Dobrin et al. (1997); Holcombe et al. (2013)]. After a rod cladding failure, fission gases that would usually be in the gas-plenum escape from the rod. Therefore there is an opportunity to assay the plenums of suspected failed rods to ascertain their γ emission. The rod which has failed would have a substantially lower γ emission in this region. When assaying the plenums, it is important to choose a fission-gas that emits γ rays of high enough energy to be detected. This is particularly relevant if a whole assembly is being assayed at the same time. For example if the 81 keV ^{133}Xe emission is chosen, then the internal rods of the assembly may not be seen (Fig. 28). In comparison the 250 keV ^{135}Xe emission can be utilised with 40

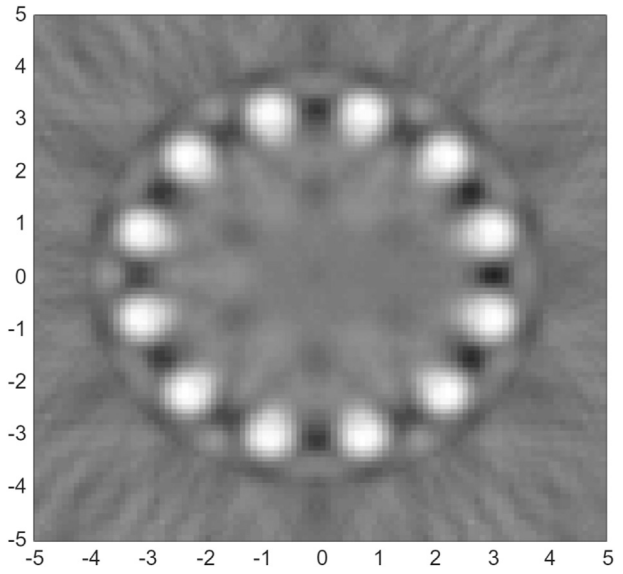

Fig. 28. A 81 keV ^{133}Xe emission simulation for a Light Water Reactor (LWR) assembly containing a failed rod. Only the peripheral rods of the assembly can be seen due the low energy of the assayed γ rays. The reconstruction was carried out using FBP [Holcombe et al. (2013)].

projections, however this method would need to be applied very early on after the assembly was removed from service as the half life of ^{135}Xe is relatively short at 9.14 h (Fig. 29).

With cladding failures costing NPPs in terms of both profits and safety, industry has endeavoured to improve cladding materials and operating conditions to reduce the chance of failures in service. As power stations continually try to increase efficiency, the options of higher burnup and longer irradiation times are routes by which to extract more power from their current fuel elements. The main barrier to this action so far is the cladding material and its physical properties. Research is ongoing into this area, usually on spent fuel, in order to gain some understanding of the state of fuel claddings

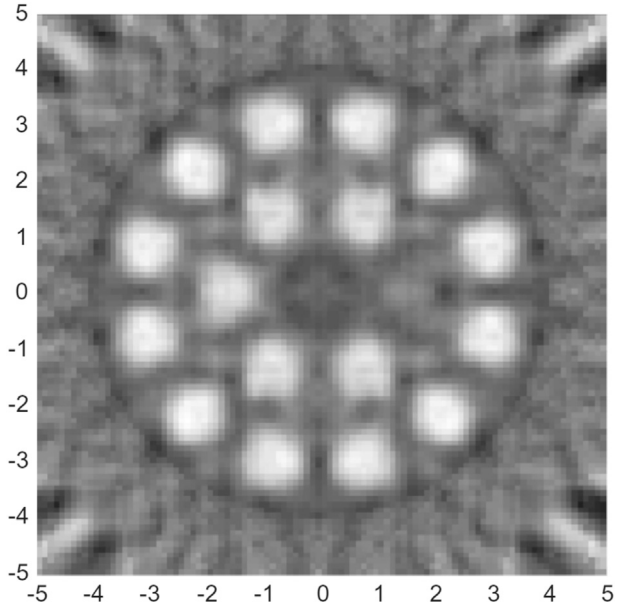

Fig. 29. A 250 keV ^{135}Xe emission simulation for a LWR assembly containing a failed rod, which is clearly visible to the right of the centre of the assembly. The reconstruction was carried out using FBP [Holcombe et al. (2013)].

after various burnup profiles [Bayon (1999); Groeschel et al. (1999)]. In these works, neutrons are used to investigate cladding instead of the usual destructive testing that has taken place in the industry so far. It can be seen in Groeschel et al. (1999) that hydrogen concentrations determined from neutron radiographs are in good agreement with the destructive *LECO hydrogen analyser*.

As with any heating element, the heat exchange surface, has to be kept clean to allow for full heat transfer. When heat transfer cannot occur, the risk of failure of the heating element (in this case the fuel rod) increases greatly. As well as the risk of failure, there is also the ever present issue of efficiency, and a rod that cannot transfer its heat correctly is reducing the efficiency of the reactor. It is carbon deposition on fuel rods, in particular, that is covered in Gras and Stanley (2008). 2D X-ray images are produced using varying X-ray energies in order to allow for visualisation of three types of carbon deposit, thin, granular or columnar (Fig. 30). Post processing enhancements such as the ImageJ algorithm (Fig. 31) and the Sobel operator (Fig. 32) are applied to the radiographs to show a more comprehensive image. For the case of carbon deposition, the ImageJ algorithm seems to give the user more ability to not only visualise but analyse quantitatively the amount of deposition on the rod.

3.2.2. Verification of spent fuels

Another reason for PIE of fuel is to verify that new types of fuel have worked as expected. Different chemical compounds used for fuel and different geometries need to be validated before they can be used in real life situations [Porter and Tsai (2012)]. For example a new MOX fuel was investigated using NDT, with the test suite including: visual examination, axial gamma scanning, leak testing, microstructural examination of fuel and cladding, fission gas analysis, $\beta-\gamma$ autoradiography and fuel central temperature estimation from restructuring. This review will only concentrate on the $\beta-\gamma$ autoradiography aspects [Sah et al. (2008)]. The autoradiographs were undertaken in order to ascertain the macrostructure of irradiated MOX pins. Samples from the centre, intermediary area and outer areas of the assembly were metallographically polished and then radiographed. There is no indication of the imaging materials used for the experiments or how they were processed. Results of these scans are shown in Fig. 33.

It is noted that the central white regions indicate the migration of radioactive fission products from the central region to the periphery of a fuel section. This would result in lower activity in the central region. It can be seen that this is more prevalent in the outer pin and least prevalent in the central pin. There is no further discussion about these images within the paper and when looked at on an individual basis they do not allow for any specific conclusions to be drawn about the fuel pins. However along with the other extensive techniques applied during the work, several conclusions about the fuel pins analysed in the paper, particularly about failure modes, were made.

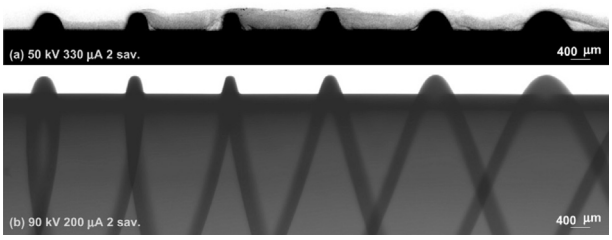

Fig. 30. 2D X-ray radiographs of coated Advanced Gas-cooled Reactor (AGR) fuel rods; a high resolution, low energy image taken at 50 kV and 330 μA (top). Higher energy X-rays, taken at 90 kV and 200 μA (bottom) [Gras and Stanley (2008)].

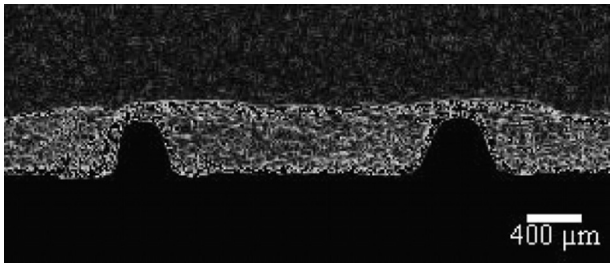

Fig. 31. A section of the X-ray radiograph in Fig. 30 after application of the image J algorithm [Gras and Stanley (2008)].

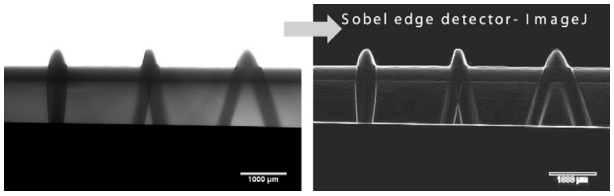

Fig. 32. A 90 kV X-Ray with its associated Sobel edge enhancement result [Gras and Stanley (2008)].

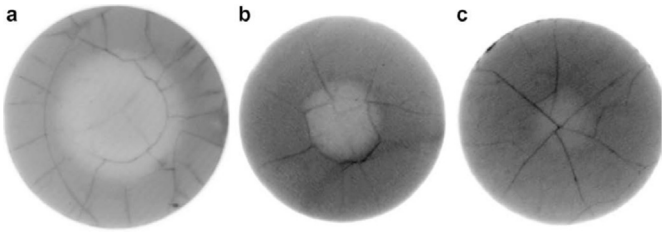

Fig. 33. $\beta - \gamma$ Autoradiographs of (a) outer, (b) intermediate and (c) central pin of a high burnup up MOX bundle [Sah et al. (2008)].

Further to verification investigations using emitted γ rays and transmission X-rays, neutron interrogation can be a valuable method by which to investigate spent fuel elements. With varying attenuation coefficients for similar Z materials, geometries of interest can be witnessed as well as differing enrichments or fuel materials. Neutron Imaging Plates (NIPs) were utilised in Yasuda et al. (2005) to carry out neutron tomography of a fuel element. In this case, work was undertaken on a fresh rod, as a feasibility test to allow a spent rod to be investigated in the near future. Fig. 34 shows the differences between an X-ray image and an NIP image. The different types of pellets, in both geometry and elemental make up, can be discerned in the neutron image, as well as greater detail about the rod components.

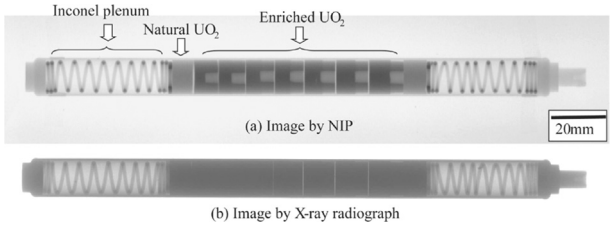

Fig. 34. A comparison of X-ray radiography against neutron imaging plate radiography. Hollows, and varying fuel materials can be discerned in the neutron image but not the X-ray image [Yasuda et al. (2005)].

In a similar vein, neutron radiography was undertaken in Sim et al. (2013), however, here it is not the image in particular that is the main point of the work. A powerful post processing tool is employed to analyse the neutron radiograph for the gap size at the fuel plug. A Horizontal/Verticle (HV) filter was utilised which allowed sharper definitions of edges of the particular region of interest. Fig. 35 shows the various stages of applying the HV filter and the associated outcome. It allows for an almost automated measurement of the gap size.

3.2.3. Accident scenarios

Accident scenarios can be seen as an extension of spent fuel analysis. This can be because it was the fuel that failed, or because the failure could have a profound effect on the fuel. Similar to the work carried out in Jonkmans et al. (2010, 2013), described earlier, muons can be used to visualise nuclear fuel materials [Sugita et al. (2014)]. This method can be particularly useful for accident scenarios such as those found in Fukushima after the 2011 nuclear disaster. In less severe accidents scenarios, damaged fuel rods can be in various physical states, from the examples seen in previous sections, where it is likely that the failures could have gone undetected by external observation to failures that are far more obvious. In this category, although investigation does not need to take place to identify the correct rod/assembly that has failed, it can be useful to glean information from the failed rod non destructively to see how the failure came about. NDT including radiography can be used to view the internals of failed rods and assemblies, whilst retaining their failure geometry.

Hansche (1989) carried out computed tomography on a failed assembly quite successfully, by digitising a number of radiographs and reconstructing them using the BKFIL filtered back projection routine with the HAN hanning window based filter, then BLL line integral based back projection. The images produced are; in comparison to images created at a similar time; very comprehensive. Various slices of the rod can be seen, and these slices have been configured to show a 3D version of the assembly (Fig. 36).

Over 20 years later very similar research is still being carried out [Biard (2013)]. Here emitted γ ray measurements along with transmission X-ray computed tomography allowed for fission product distributions to be evaluated. In comparison to the work done by Hansche (1989), there is no 3D reconstruction of the fuel bundle, but there are various 2D reconstructions (Fig. 37), which show different isotopes. It can be seen from these images, where failure has occurred. This image shows all isotopes, which was the first step of the work. Following this, data were extracted for each isotope at a given location which allowed tomograms of each isotope to be produced after self-attenuation correction had been computed.

Again, it is not just geometries of fuel that can be ascertained with radiography. Elements such as hydrogen can be viewed by neutron interrogation. During a Loss Of Coolant Accident (LOCA) hydrogen is produced when water is re-injected to the core, this is then free to chemically react with items in the nuclear reactor. If it reacts with the zircalloy cladding, it can cause embrittlement [Allen et al. (2012)] which may lead to catastrophic failure of the rods. Research has been undertaken to quantify hydrogen take up in zircalloy after simulated LOCA conditions. Naturally, this was done with neutrons due the differing attenuation of neutrons during hydrogen and zircalloy interrogation [Grosse et al. (2008, 2011a, 2011b, 2012, 2013); Jenssen et al. (2014)]. In the cited work carried out by Grosse, hydrogen uptake is calculated by measuring the attenuation and using the H/Zr ratio. The ratios are calibrated in the first instance and show good correlation to measured data. Fig. 38 shows varying H/Zr ratios, even ratios as close as 0.279 and 0.23 can be discerned. For the first time, the hydrogen concentration in Zircalloy cladding can be determined *in-situ*. This could allow NPPs to assess their fuel assemblies quantitatively to provide valuable safety data about the state of the assemblies. It also allows for more understanding of the effects of rod location on hydrogen uptake, which would appear to vary according to the study.

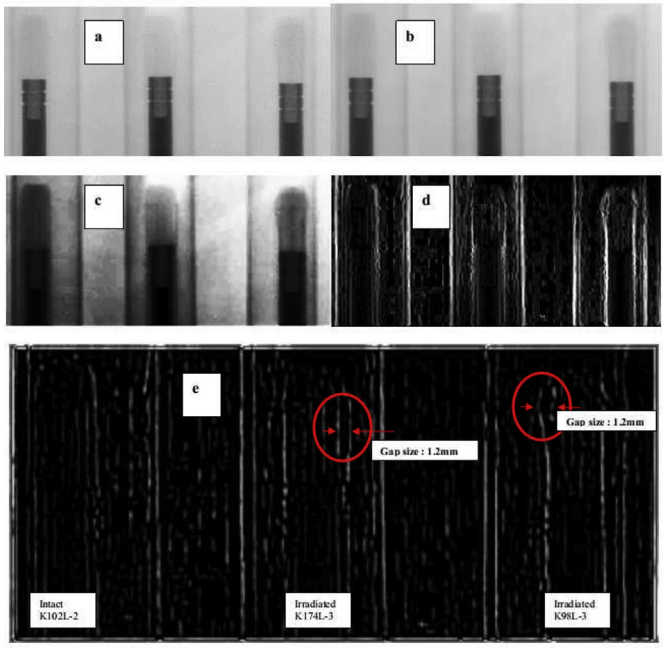

Fig. 35. Neutron radiographs at varying stages of post processing in order to calculate the size of the ballooning gap. (a) Original image, (b) Noise reduced image created using median filter, (c) Enhanced image created using histogram equalisation method, (d) Image after Sobel operator using verticle filter-1, (e) Laplacian Gaussian image of the three spent fuel rods with associated plugs [Sim et al. (2013)].

4. Improvements to nuclear fuel

Improvements in safety and cost are always sought after in an industry where great expense is required at every stage of the process. Improving fuel use and efficiency could save NPP operators

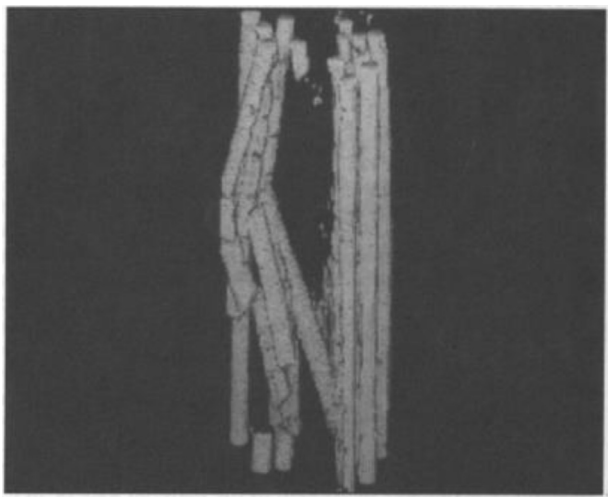

Fig. 36. A 3D FBP reconstruction of a failed LWR assembly from digitised radiographs [Hansche (1989)].

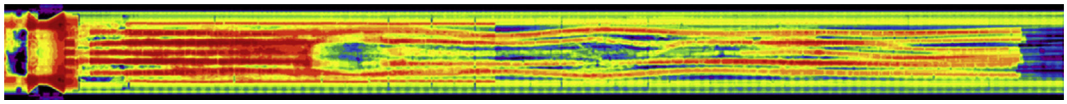

Fig. 37. Barium distribution throughout a failed FPT3 assembly. Reconstructed using FBP [Biard (2013)].

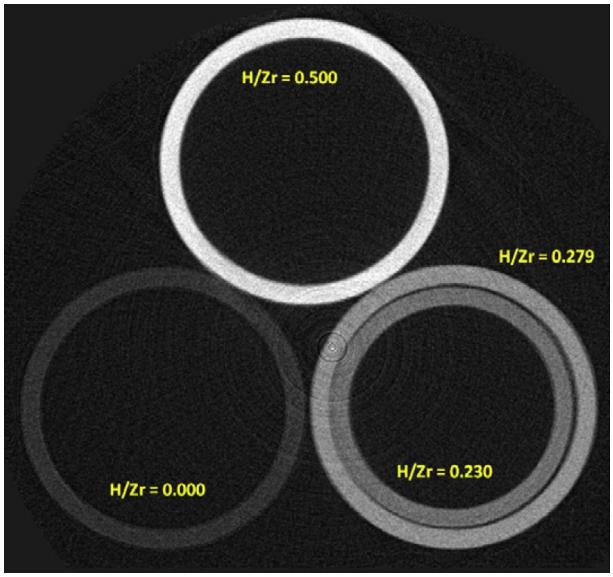

Fig. 38. A neutron tomograph showing various H/Zr ratio cladding tubes. 0.23 and 0.279H/Zr ratios can easily be differentiated [Grosse et al. (2013)].

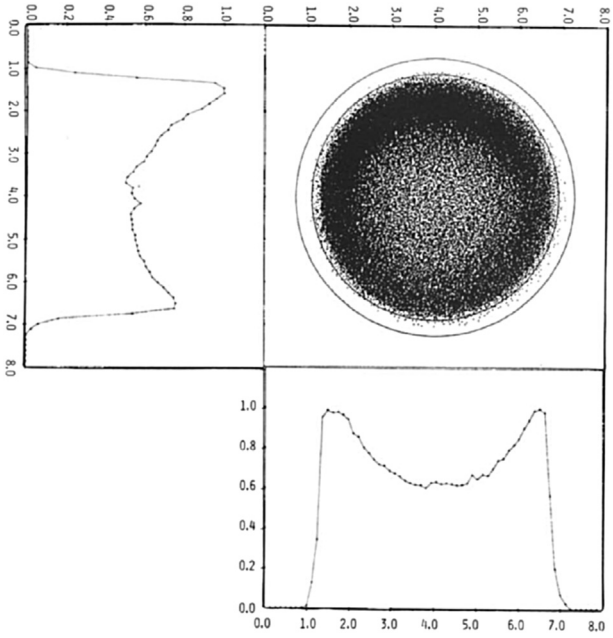

Fig. 39. A 2D gamma scan for ^{103}Ru (496.9 keV) of a fuel pin and the resulting reconstructed 2D density plot [Barnes et al. (1979)].

a great deal of money and allow for either greater profit margins, or a reduction in cost to the consumer. Most research in this area is concerned with burnup and isotope distribution. As mentioned earlier, longer burnup times and higher temperature burnups are seen as a possible way of increasing efficiency. In the previous section the main aim of the research work was to investigate the cladding materials during high or long burnup. Investigations into the fuel material itself is also an important parameter when it comes to investigating burnup and the following section will provide an insight into research carried out to date in the field of imaging using radiation [Berzins et al. (1981); Lundqvist et al. (2010)].

Detection and spectroscopy of γ rays is a well studied technique, particularly for emitted γ rays. The method of detecting emitted γ rays allows for the identification of specific isotopes present in the fuel by narrowing the band within which γ rays are detected. When tomography is used the full cross sectional distribution of certain isotopes can be determined. One of the earliest images produced using emitted γ rays to show isotope distribution can be seen in Barnes et al. (1979). The 2D scan is composed of two scans of the same diametral portion of an item which are reconstructed to show a possible 2D distribution of the assayed item. Fig. 39 is the reconstructed image of two ^{103}Ru (496.9 keV) scans of the same diametral section of irradiated fuel pin at 0° and 90° respectively.

This image has been reconstructed in a similar way to conventional medical tomography. However, the algorithms used here allow for a reduction from 200 measurements at 180 angular positions to just one measurement at two angular positions. Barnes states that comparisons between these reconstructed density plots and data retrieved from sectioned fuel pins show better spatial resolution than medical tomography which, at the time, worked to roughly 1 cm. The huge reduction in positions and measurements would be a major advantage over the medical tomography that Barnes uses as a comparison. The reduction relies heavily on the general symmetry of fuel pins, however the paper does not contain any images produced by medical tomography for comparison so it difficult to judge how similar the images really would be.

Similar work has been carried out since [Ducros (1985); Hofmann et al. (1988); Alexa et al. (1995); Niculae et al. (1996); Pan and Tsao (1999); Svard et al. (2005)], mostly producing tomographs of specific isotope distributions at distinct locations

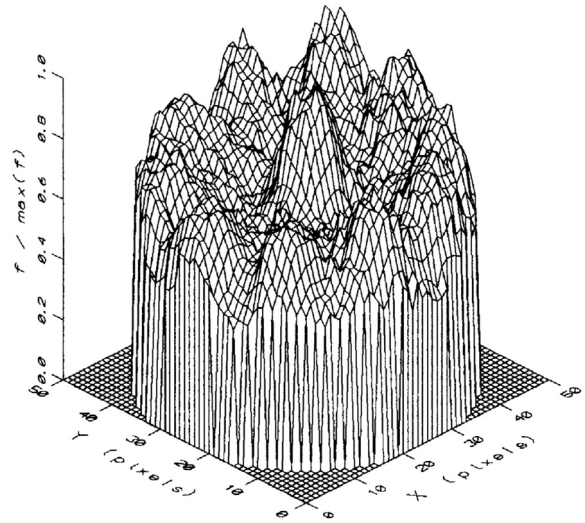

Fig. 40. Diametral distribution of ^{140}La (1596 keV) in a fuel pin. Reconstruction was carried out using the Maximum Likelihood technique [Niculae et al. (1996)].

along a spent fuel pin. An example has been shown in Fig. 40 of the distribution of ^{140}La throughout a rod. From the raw data, ratios of isotopes such as ^{134}Cs and ^{137}Cs which can be used to approximate neutron distribution better than either isotope alone [Pan and Tsao (1999)].

Extensive research into very high burnups has been carried out at the Paul Scherer Institute in Switzerland. Ratios of ^{134}Cs, ^{137}Cs and ^{154}Eu were determined [Caruso et al. (2008a, 2009); Caruso and Jatuff (2014)]. Previously investigations had concentrated on lower burnup fuels. Alongside this work comparisons between fuel density and burnup profiles were being carried out using transmitted and emitted neutrons [Caruso et al. (2008b)]. The work shows a linear relationship between burnup and density of the fuel, even after the already understood densification period observed in the early stages of irradiation. With more calibration, density profiles could be utilised for estimating burnup making use of γ transmission. Fig. 41 shows how the density of a rod changes with increasing burnup.

It is interesting to note that in the works shown here, the attenuation matrix used to create the tomographs has been derived experimentally rather than by simulation. The matrix was produced using gamma transmission tomography and then utilised for Single-Photon Emission Computed Tomography (SPECT) reconstruction. This method can produce highly accurate results as the morphology of the sample is taken into account within the matrix.

Reaction rates including fission rates and capture rates can be useful to reduce the effect of self absorption during γ emission tomography. Fauchere et al. (2004) makes use of the total fission rate (F_{tot}) and the capture rate in ^{238}U (C_8). These values are processed to give a correction factor to be used in pin-integral measurements. It is claimed in Oleinik et al. (2005) that tomography during re-fuelling could glean far more information than the current method of estimating burnup from measurements of γ radiation. If the technique could allow for better understanding of the fuel's state, without a much greater cost or time then it may seem like a very good idea. A facility to measure these types of data is described in Kotiluoto et al. (2009), with the major theme of the work centering around the detector response. A High-Purity Germanium (HPGe) detector is simulated to ensure that sufficient data are available after both emission and transmission tomography. Facilities like this would vastly reduce the amount of destructive testing that currently goes on in the nuclear industry, thus working more safely and saving money.

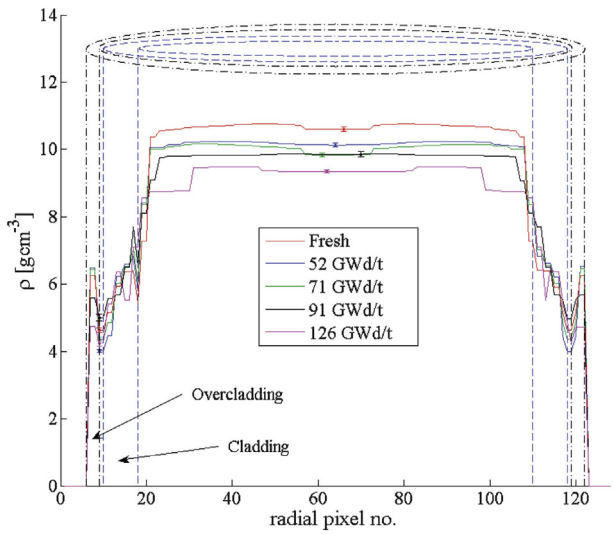

Fig. 41. Varying densities with increasing burnup scenarios [Caruso et al. (2008b)].

Neutrons have also been investigated for use in determining fission product distribution [Cason and Jackson (1971); Tanke et al. (1991)]. The former using transmission neutrons and the later detecting emitted neutrons from spent fuel. Cason uses an indium foil and then converts the resultant radiograph into a density graph using a densitometer. This method does not seem to lend itself well to being able to identify fission product distribution, and in fact there is no mention about how this would be done, just the radiograph as the result. Using emitted neutrons on the other hand allows for more information about fissile materials, particularly those undergoing spontaneous fission.

5. Post processing techniques

In addition to the physical detection of radiation for imaging purposes, there are numerous numerical and post processing methods that are useful during imaging of nuclear fuels. These range from mathematical models that can be used to help set up imaging scenarios [Panakkal et al. (1986)] to assessing pebble-bed reactor layouts to investigate flow [Auwerda et al. (2013)].

One of the most obvious differences between tomographic images in particular is the reconstruction technique. This issue is addressed in Barton (1977); Honda et al. (1990) and Craciunescu et al. (1995). Neutron interrogation is used in the two former articles, with Barton (1977) comparing differing numbers of angles and projections in ART reconstruction in a feasibility study. Examples of images produced are provided, but are unsuitable for reproducing here. It is concluded that ART is better suited to high contrast objects than convolution methods which is in stark contrast to Honda et al. (1990). The latter stating that Convolution Integral (CI) was preferred in comparison to Fourier Transform (FT) [Lim (1990)], Filtered Back Projection (FBP) [Bruyant (2002)] and Maximum Entropy (ME) [Skilling and Bryan (1984)]. Neither paper provides quantitative data upon which to base their arguments about which technology is more suited to the problem. Unlike Craciunescu et al. (1995), here four methods of gamma emission tomography are compared in a simulator to ascertain which is more suited to evaluating burn-up within the fuel. The work presented utilised two phantoms and then simulated the scanning of these phantoms using the following methods: Maximum Likelihood (ML), Maximum Entropy (ME), ART, and Monte Carlo implementation of the Back Projection Technique (MCBP).

The phantoms utilised are shown in Figs. 42 and 43.

Comparisons were made about the different techniques not just by the quality of their output but also by the method itself i.e. the computational equipment required or the length of time the method takes in practice. All of these characteristics are pertinent when choosing a scanning technique. Table 1 documents the results of the simulations carried out.

The discussion in the paper also presents the chi-squared and correlation coefficient of each of the methods in order to quantify each method. It shows that the ML method creates the closest reconstruction with ME, ART and MCBP following respectively. However, the ML method requires a large computing time due to the mathematics involved, so if time is a factor in the requirements the ME method would be more suitable. The results observed will provide future researchers with a good starting point when deciding what kind of tomography to use for differing projects.

Similar to work presented earlier, Caruso et al. (2009) compares various reconstruction techniques to identify the fission product profiles of UO_2 fuel at varying levels of burnup. The reconstruction techniques include: FBP, Penalised maximum-Likelihood expectation maximisation in the form of Space-Alternating GEneralised

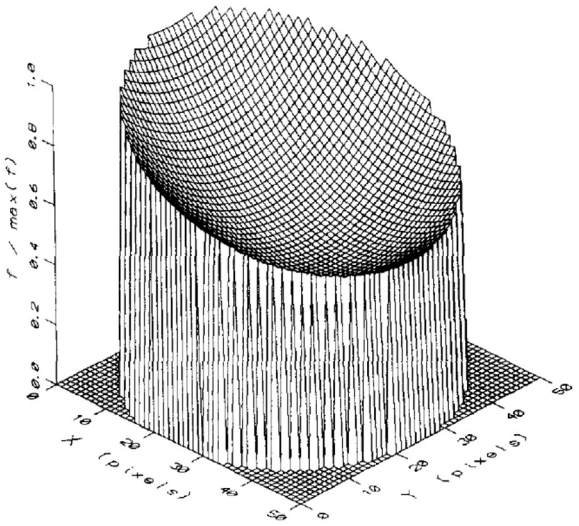

Fig. 42. Phantom 1 used by Craciunescu to simulate various tomography techniques [Craciunescu et al. (1995)].

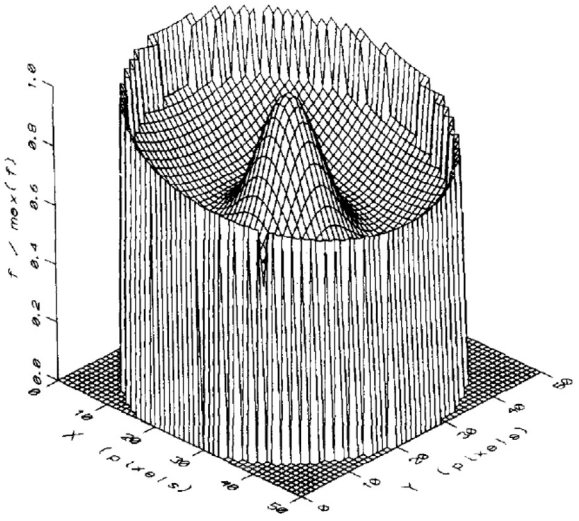

Fig. 43. Phantom 2 used by Craciunescu to simulate various tomography techniques [Craciunescu et al. (1995)].

(PL-SAGE), ordered subset De Pierro (PL-DP), Penalised Weighted Least Square (PWLS) and Paraboloidal Surrogates Coordinate Ascent (PSCA). A phantom is used in the first instance to identify the most suitable reconstruction technique. The reconstruction techniques are simulated and the results produced can be seen in Fig. 44.

A quantitative comparison is carried out using a figure of merit which concludes that of these techniques PSCA produces the finest image, followed by PL-DP, PWLS, PL-SAGE and FBP respectively. The PSCA algorithm is then used to reconstruct experimental data for the four burnt pellets. The image produced (Fig. 45) shows how the concentration across the fuel cross section of ^{134}Cs varies with burnup. There are similar images produced of ^{137}Cs and ^{154}Eu.

These techniques are mathematical in nature and in more recent years, computing has brought around a number of different ways of logic manipulation. Craciunescu (2004) makes use of a neural network to reconstruct fission product distribution. Neural networks are algorithms that dictate statistical learning. They can handle a large number of inputs and are adaptive. Both of these qualities make for a good reconstruction algorithm, particularly if one is using a large number of projections, for example in the case of a 3D image.

6. Discussion

A review of the imaging of nuclear fuel using ionising radiation has been presented. The work has been categorised using the aims presented by each author and broadly separates into Safeguarding, Quality Assurance and improvements to nuclear fuel. Any comments or discussions that are specific to a paper are included above, and following will be a broad overview at imaging in the nuclear industry moving forwards and future work that may prove useful.

The easiest parameters of imaging nuclear fuel with ionising radiation to improve are; reduction in assay times and higher resolution images. Lower assay times may be achieved with higher efficiency detectors, changes in collimation setup and better counting statistics. Higher resolution may be achieved by obtaining more projections and using more suitable reconstruction techniques.

It can be seen from the results obtained over the majority of the papers that black and white images that portray density of fissile material are very well understood. There has been sporadic improvement in this area, with developments such as those described in Tamaki et al. (2005). The paper describes a new radiography technology for dysprosium sheet imaging, whereby transfer of the dysprosium film onto an x-ray film does not need to occur. However, it can be argued that with the depth of knowledge already available in the medical sector regarding tomography and 3D imaging, there is little advancement that can be made in the nuclear sector in the short term. It is recommended that the two types of technology are combined in order to continue work similar to that of Hausladen (2013) and Lehmann et al. (2003).

Higher resolution and 3D images can be achieved with new or improved reconstruction techniques. Previous works that are not specific to nuclear fuel can be seen in Fessler (1994); Fessler and Hero (1994); De Pierro (1995); Erdogan and Fessler (1999), and Sotthivirat and Fessler (2002) to name but a few. Research continues in this field, for both medical imaging and mathematical data processing. For example, a new method called compressed sensing (CS) has recently been proven [Je et al. (2014)] which suggests that far fewer projections can be used to create images of a resolution on par with images produced by current methods. The CS method works on the basis of optimising signals that are sparse using data about how sparse the signal is. It is shown that if fewer images can produce the same resolution, then the same amount of images used in current reconstruction methods produce higher resolution images. Overall assay times for imaging could be reduced as the information produced becomes more useful. Reconstruction techniques like this will allow images to be taken of nuclear fuel and SNM in shorter times and therefore possibilities are introduced, such as, in-line imaging during manufacture or 100% imaging of spent fuel assemblies at NPPs after irradiation.

The use of various reconstruction techniques in the papers presented makes direct comparison between them difficult. Further to the work carried out to identify the best reconstruction algorithms [Craciunescu et al. (1995); Honda et al. (1990)] there is room for a more indepth analysis of what type of reconstruction is more ideal for certain situations.

As well as processing techniques, a number of new imaging facilities are being designed and built [Gaillot et al. (2008); Cortesi et al. (2012); Parrat et al. (2013); Wei et al. (2013)]. The ones mentioned here are neutron imaging facilities, there are a few possible reasons for this. Firstly, as can be seen in the images above, neutrons can be used to produce a far more penetrative image of

Table 1
Comparison of Craciunescu's four methods of tomography simulating γ rays on spent fuel [Craciunescu et al. (1995)].

Processor	Phantom 1	Phantom 2
Maximum Likelihood (ML)	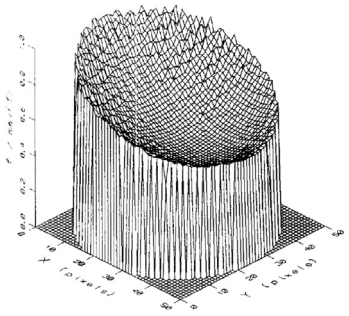	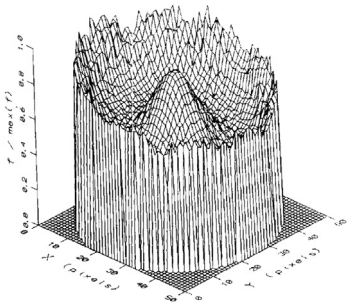
Maximum Entropy (ME)	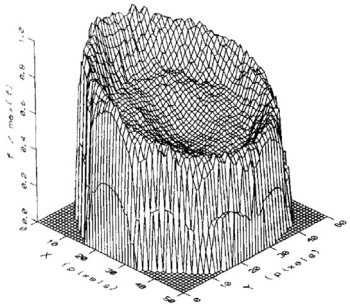	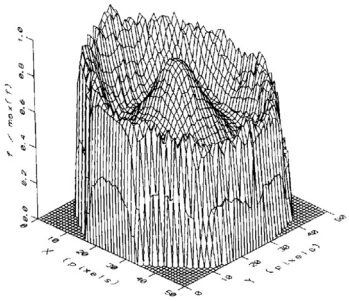
Algebraic Reconstruction Technique (ART)	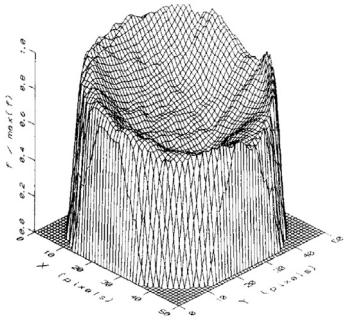	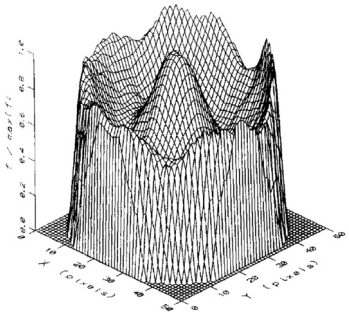
Monte Carlo Implementation of the Back Projection technique (MCBP)	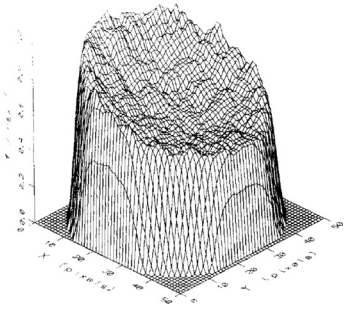	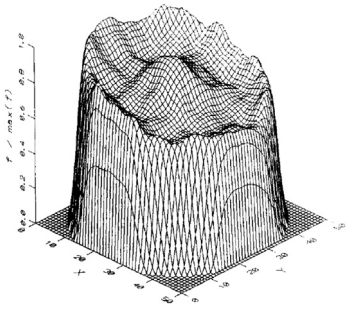

nuclear fuel than any of the other radiations discussed. Further examples are provided in Ross (1977) and Domanus (1984). Secondly, as time progresses our understanding of neutron production and detection is increasing, and has vastly been expanded in the last five decades. With the introduction of CCD cameras and scintillation detectors, neutrons can now be imaged much more easily than they used to be. With an increase in neutron imaging facilities, there will also be more opportunity to improve detection efficiency of neutrons with new technology. It is also apparent that neutrons are being used to interrogate non-nuclear items, and as the engineering industry as a whole realises the benefits of neutron imaging, there may be an increase in workloads at neutron imaging facilities [Pleinert et al. (1994)].

Neutron detection is an area that would benefit from improvement. At the time of writing, neutrons cannot be detected directly. They are usually detected indirectly by their interaction with matter. In the case of scintillation detection, for example, they are detected along with γ rays, and post processing has to take place to discern γ rays from neutron incidents. There has been a body of work which has improved this technique, and now the separation of radiation events can be done almost instantaneously, but there is still uncertainty surrounding the results as at lower amplitudes the γ ray and neutron data can overlap. Possible improvements in

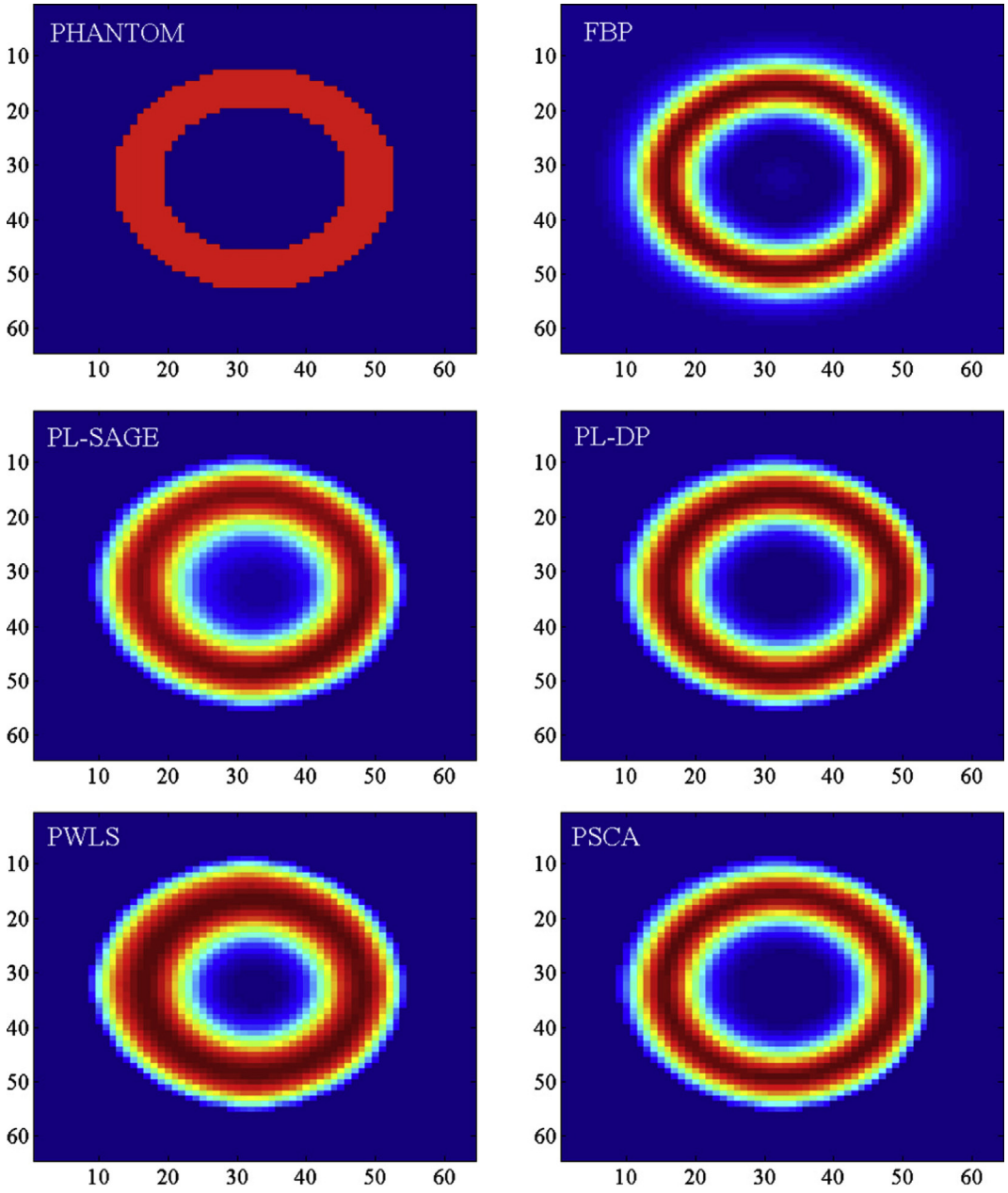

Fig. 44. Reconstructions of a simulated phantom using various techniques. The phantom is shown in the top-left image, with the reconstructions following, and labelled as per their reconstruction technique [Caruso et al. (2009)].

neutron detection have been researched, such as Sanders et al. (2002), which describes a system that utilises Gallium-Arsenide (GaAs) detectors to carry out neutron computed tomography. The GaAs detectors are smaller than conventional CCD detector set-ups and according to Sanders et al., give better resolution of hard components too. It would be highly beneficial for further research into neutron imaging to continue, particularly to devise a method to directly detect, or detect with much lower uncertainties, the presence of neutrons.

One method that is under utilised thus far is the use of fission neutrons, both as interrogating radiation, and as emitted radiation to be measured. Bucherl et al. (2011) describes a new facility that hopes to do just this using two plates of highly enriched uranium (HEU) activated by a beam tube from the Forschungs Neutronenquelle Heinz Maier–Leibnitz (FRM II). Fast neutron detection can be carried out by modern detectors and thus, radiography and tomography at this facility may produce some interesting results, not seen before.

There is a lack of instrumentation verified for use to identify partial and bias defects in both fresh and spent fuel Fritzell and Kautsky (2010) so it would be advantageous to further research in these areas. Also QA will need updating as the nuclear industry is potentially looking towards a more diverse set of fuel materials [Crossland (2012)]. This could include more thorium based fuels, higher burn-up fuels and hydride fuels. All of which would need a level of reliability similar to those fuels already in use. Nuclear imaging could provide a comparatively easy and cheap method of assaying fabricated fuel. Automatic and continuous material detection is likely to be a future step for nuclear fuel imaging, and SNM in general. As more underground repositories are built, it is

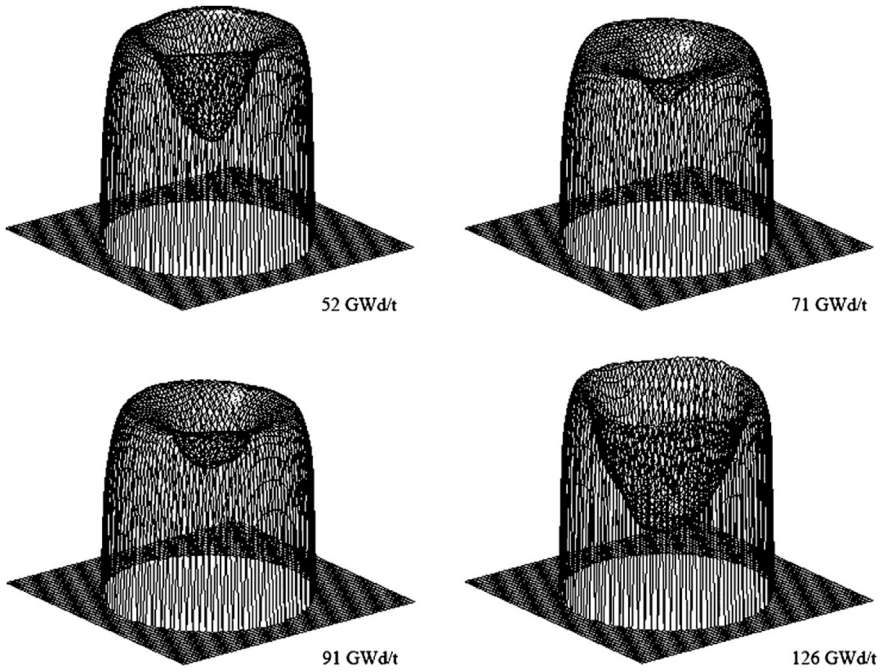

Fig. 45. 3D γ tomographs of the ^{134}Cs within-rod distributions of four fuel rods with varying burnup profiles. The images are reconstructed using the 795 keV γ peak [Caruso et al. (2009)].

likely that the entombed spent fuel will be increasingly monitored as monitoring becomes more affordable. This may ensure COK of SNM, and provide an extra level of safety too.

That said, there is a discussion to be had around material accountancy and when enough is enough. For example, during fuel manufacture there will be an amount of SNM that is lost or trapped within the machinery. This is known in the nuclear industry as Material Unaccounted For (MUF), and is an accepted inevitability. To this end, the COK data will always have losses, and so, it may be argued that a bias defect is something that could be accepted too. If an person wanted to remove small amounts of SNM from the production line, there are routes available and over time, lots of small diversions could add up to a large amount of SNM being diverted. Maybe it is here that more effort should be concentrated? In principle, different and often greater challenges exist to remove nuclear material from a rod or assembly, than those that must be overcome to remove it from the pelletisation and sintering phase of manufacture.

An improvement in imaging technology could greatly improve fuel safety as well as PIV of nuclear fuel at various points within the fuel cycle when utilised appropriately, thus the safety benefits of advancement could be twofold.

Acknowledgements

The authors would like to acknowledge the financial support given by the Engineering and Physical Sciences Research Council (EPSRC) and Lancaster University.

References

Alexa, A., Craciunescu, T., Mateescu, G., Dobrin, R., Feb. 1995. The tomographic maximum entropy method in the 3-D analysis of nuclear fuel pins. J. Nucl. Mater. 218 (2), 139–142. URL. http://www.sciencedirect.com/science/article/pii/0022311594004358.

Allen, T.R., Konings, R.J.M., Motta, A.T., 2012. Corrosion of zirconium alloys. Compr. Nucl. Mater. 49–68.

Auwerda, G.J., Kloosterman, J.-L., Lathouwers, D., Van der Hagen, T.H.J.J., Sep. 2013. Macroscopic and microscopic packing properties of experimental and computational pebble beds. Nucl. Technol. 183 (3), 272–286 wOS:000323689000002.

Baghra, C., Sathe, D.B., Prakash, A., Mishra, A.K., Afzal, M., Panakkal, J.P., Kamath, H.S., 2013. Characterization and property evaluation of (Th–3.75U) O_{2+x} fuel pellets fabricated by impregnated agglomerate pelletization (IAP) process. Nucl. Eng. Des. 259 (0), 113–117. URL. http://www.sciencedirect.com/science/article/pii/S0029549313001088.

Bakker, J., Baritello, A., Bordo, J., Markgraf, J.F.W., Leeflang, H.P., Ruyter, I., Jan. 1987. Neutron radiography of light water reactor fuel rods at the high flux reactor petten. Neutron Radiogr. Springer Neth. 381–393. URL. http://link.springer.com/chapter/10.1007/978-94-009-3871-7_49.

Barnes, B., Phillips, J., Waterbury, G., Quintana, J., Netuschil, J., Murray, A., 1979. Characterization of irradiated nuclear fuels by precision gamma scanning. J. Nucl. Mater. 81 (1–2), 177–184. URL. http://www.scopus.com/inward/record.url?eid=2-s2.0-0017951751&partnerID=40&md5=e3dc54a0f237c5284e36627a50d126da.

Barton, C., 1977. Computerized axial tomography for neutron radiography of nuclear-fuel. Trans. Am. Nucl. Soc. 27 (NOV), 212–213 wOS: A1977EB66000637.

Bayon, G., Nov. 1999. Present applications of neutron radiography in France. Nuclear instruments and methods in physics research section a: accelerators, spectrometers. Detect. Assoc. Equip. 424 (1), 92–97. URL. http://www.sciencedirect.com/science/article/pii/S016890029801242X.

Behrens, J., Schrack, R., Carlson, A., Bowman, C., 1979. Resonance neutron radiography for nondestructive assay of fresh nuclear-reactor fuel. Bull. Am. Phys. Soc. 24 (7), 874–875 wOS: A1979HN33400355.

Berzins, G.J., McKinnon, G.C., Bates, R.H.T., Lumpkin, A.H., Apr. 1981. Application of computed tomography techniques to pinhole images of nuclear-reactor test fuel rods. Nucl. Sci. Eng. 77 (4), 493–495. URL. http://epubs.ans.org/?a=18962.

Biard, B., Sep. 2013. Quantitative analysis of the fission product distribution in a damaged fuel assembly using gamma-spectrometry and computed tomography for the Phébus FPT3 test. Nucl. Eng. Des. 262, 469–483. URL. http://www.sciencedirect.com/science/article/pii/S0029549313002823.

Brenizer, J.S., 2013. A review of significant advances in neutron imaging from conception to the present. Phys. Procedia 43, 10–20. URL. http://www.sciencedirect.com/science/article/pii/S1875389213000163.

Brown, D.W., Balogh, L., Byler, D., Hefferan, C.M., Hunter, J.F., Kenesei, P., Li, S.F., Lind, J., Niezgoda, S.R., Suter, R.M., Feb. 2014. Demonstration of near field high energy X-ray diffraction microscopy on high-Z ceramic nuclear fuel material. Mater. Sci. Forum 777, 112–117. URL. http://www.scientific.net/MSF.777.112.

Bruyant, P.P., Oct. 2002. Analytic and iterative reconstruction algorithms in SPECT. J. Nucl. Med. 43 (10), 1343–1358. URL. http://jnm.snmjournals.org/content/43/10/1343.

Bucherl, T., Lierse von Gostomski, C., Breitkreutz, H., Jungwirth, M., Wagner, F.M., Sep. 2011. NECTARA fission neutron radiography and tomography facility. Nucl. Instrum. Methods Phys. Res. Sect. A Accel. Spectrom. Detect. Assoc. Equip. 651 (1), 86–89. URL. http://www.sciencedirect.com/science/article/pii/S0168900211001367.

Caruso, S., Gnther-Leopold, I., Murphy, M.F., Jatuff, F., Chawla, R., May 2008a. Comparison of optimised germanium gamma spectrometry and multicollector inductively coupled plasma mass spectrometry for the determination of ^{134}Cs, ^{137}Cs and ^{154}Eu single ratios in highly burnt UO_2. Nucl. Instrum. Methods Phys. Res. Sect. A Accel. Spectrom. Detect. Assoc. Equip. 589 (3), 425–435. URL. http://www.sciencedirect.com/science/article/pii/S0168900208003513.

Caruso, S., Jatuff, F., Apr. 2014. Design, development and utilisation of a tomography station for gamma-ray emission and transmission analyses of light water reactor spent fuel rods. Prog. Nucl. Energy 72, 49–54. URL. http://www.sciencedirect.com/science/article/pii/S0149197013001856.

Caruso, S., Murphy, M.F., Jatuff, F., Chawla, R., 2008b. Nondestructive determination of fresh and spent nuclear fuel rod density distributions through computerised gamma-ray transmission tomography. J. Nucl. Sci. Technol. 45 (8), 828–835. URL. http://www.tandfonline.com/doi/abs/10.1080/18811248.2008.9711484.

Caruso, S., Murphy, M.F., Jatuff, F., Chawla, R., Jul. 2009. Determination of within-rod caesium and europium isotopic distributions in high burnup fuel rods through computerised gamma-ray emission tomography. Nucl. Eng. Des. 239 (7), 1220–1228. URL. http://www.sciencedirect.com/science/article/pii/S0029549309001344.

Cason, J., Jackson, C., 1971. Neutron radiography for nuclear fuel interrogation. Trans. Am. Nucl. Soc. 14 (2), 538–&, wOS: A1971L983300138.

Cortesi, M., Zboray, R., Adams, R., Dangendorf, V., Prasser, H.-M., Feb. 2012. Concept of a novel fast neutron imaging detector based on THGEM for fan-beam tomography applications. J. Instrum. 7 (02), C02056. URL. http://iopscience.iop.org/1748-0221/7/02/C02056.

Craciunescu, T., 2004. A neural network model for the tomographic analysis of irradiated nuclear fuel rods. Nucl. Technol. 146 (1), 65–71. URL. http://cat.inist.fr/?aModele=afficheN&cpsidt=15801248.

Craciunescu, T., Niculae, C., Mateescu, G., Turcanu, C., Sep. 1995. A comparison of four tomographic methods for nuclear fuel pin analysis. J. Nucl. Mater. 224 (3), 199–206. URL. http://www.sciencedirect.com/science/article/pii/0022311595000844.

Crossland, I., Sep. 2012. Nuclear Fuel Cycle Science and Engineering. Elsevier.

Dande, Y.D., Ghosh, J.K., Panakkal, J.P., Nov. 1991. Neutron radiography at ASPARA reactor. Indian J. Pure Appl. Phys. 29 (11), 721–731.

Davies, G., Spyrou, N.M., Hutchinson, I.G., Huddleston, J., Jan. 1986. Applications of emission tomography in the nuclear industry. Nucl. Instrum. Methods Phys. Res. Sect. A Accel. Spectrom. Detect. Assoc. Equip. 242 (3), 615–619. URL. http://www.sciencedirect.com/science/article/pii/0168900286904766.

De Pierro, A., Mar. 1995. A modified expectation maximization algorithm for penalized likelihood estimation in emission TomorzraDhv. IEEE Trans. Med. Imaging 14 (1), 132–137.

Devlin, D., Jarvinen, G., Patterson, B., Pattillo, S., Valdez, J., Liu, X.Y., Phillips, J., Nov. 2009. New generation nuclear fuel structures: dense particles in selectively soluble matrix. J. Nucl. Mater. 394 (23), 190–196. URL. http://www.sciencedirect.com/science/article/pii/S0022311509007922.

Dobrin, R., Craciunescu, T., Tuturici, I.L., Jul. 1997. The analysis of failed nuclear fuel rods by gamma computed tomography. J. Nucl. Mater. 246 (1), 37–42. URL. http://www.sciencedirect.com/science/article/pii/S0022311597000421.

Domanus, J.C., Jan. 1984. Contents of the Collection. In: Domanus, J.C. (Ed.), Reference Neutron Radiographs of nuclear reactor fuel/Neutronogrammes de Reference pour le combustible nuclaire. Springer, Netherlands, pp. 16–29. URL. http://link.springer.com/chapter/10.1007/978-94-009-6337-5_7.

Doyle, J., Apr. 2011. Nuclear Safeguards, Security and Nonproliferation: Achieving Security with Technology and Policy. Elsevier.

Ducros, G., 1985. ISARD, a Method of Tomographic Reconstruction of the Position of Gamma Emitters in a Nuclear Fuel Pin from Transversal Gamma Scanning, p. 68. URL. http://www.scopus.com/inward/record.url?eid=2-s2.0-0022027866&partnerID=40&md5=70575455c9e0f77502348f50025967ba.

Erdogan, H., Fessler, J.A., Jul. 1999. Ordered subsets algorithms for transmission tomography. Phys. Med. Biol. 44, 2835–2851.

Fauchere, C.P., Jatuff, F., Murphy, M., Chawla, R., Apr. 2004. Adapting and applying SPECT to the investigation of reaction rate distributions within lightly activated nuclear fuel pins. Nucl. Instrum. Methods Phys. Res. Sect. A Accel. Spectrom. Detect. Assoc. Equip. 522 (3), 579–590. URL. http://www.sciencedirect.com/science/article/pii/S016890020303314X.

Fessler, J., Jun. 1994. Penalized weighted least-squares image reconstruction for positron emission tomography. IEEE Trans. Med. Imaging 13 (2), 290–300.

Fessler, J.A., Hero, A.O., Oct. 1994. Space-alternating generalized expectation-maximization algorithm. IEEE Trans. Signal Process. 42 (10), 2664–2677.

Fritzell, A., Kautsky, F., 2010. On the Requirement for Partial Defect Measurements Prior to Final Disposal of Spent Nuclear Fuel. URL. http://inis.iaea.org/Search/search.aspx?orig_q=RN:42081527.

Gaillot, S., Guigon, A., Cathalau, S., Parrat, D., Bayon, G., 2008. In-pool Neutron Radiography for the Jules Horowitz Reactor: a Key Non Destructive Equipment Project within a Modern Experimental Process. Destech Publications, Inc, Lancaster wOS:000260456500009.

Ghosh, J., Chandrasekharan, K., Subramanian, A., Patil, B., Purushotham, D., Panakkal, J.P., 1997. Neutron Radiography of Nuclear Fuel Pins: an Album. Engineering (E1700) 29045478. Bhabha Atomic Research Centre, India. URL. http://inis.iaea.org/search/search.aspx?orig_q=RN:29045478#.

Ghosh, J.K., Panakkal, J.P., Chandrasekharan, K.N., Subramanian, A., Roy, P.R., 1983a. Penetrating Radiation as a Tool for Quality Evaluation of Nuclear Fuels. Engineering (E1700), General Studies of Nuclear Reactors (E2300) 16034971. India. URL. http://inis.iaea.org/search/search.aspx?orig_q=RN:16034971.

Ghosh, J.K., Panakkal, J.P., Roy, P.R., 1983b. Monitoring plutonium enrichment in mixed-oxide fuel pellets inside sealed nuclear fuel pins by neutron radiography. NDT Int. 16 (5), 275–276. URL. http://www.sciencedirect.com/science/article/pii/030891268390127X.

Ghosh, J.K., Panakkal, J.P., Roy, P.R., 1984. Use of autoradiography for checking plutonium enrichment and agglomerates in mixed-oxide fuel pellets inside welded fuel pins. NDT Int. 17 (5), 269–271. URL. http://www.sciencedirect.com/science/article/pii/030891268490186X.

Gordon, R., Jun. 1974. A tutorial on art (algebraic reconstruction techniques). IEEE Trans. on Nucl. Sci. 21 (3), 78–93.

Gozani, T., Jan. 1981. Active Nondestructive Assay of Nuclear Materials: Principles and Applications. Tech. Rep. NUREG/CR-0602; SAI-MLM-2585. Science Applications, Inc, Palo Alto, CA (USA). Monsanto Research Corp., Miamisburg, OH (USA). Mound. URL. http://www.osti.gov/scitech/biblio/6215952.

Gras, C., Stanley, S.J., May 2008. Post-irradiation examination of a fuel pin using a microscopic X-ray system: measurement of carbon deposition and pin metrology. Ann. of Nucl. Energy 35 (5), 829–837. URL. http://www.sciencedirect.com/science/article/pii/S0306454907002654.

Groeschel, F., Schleuniger, P., Hermann, A., Lehmann, E., Wiezel, L., Nov. 1999. Neutron radiography of irradiated fuel rod segments at the SINQ: loading, transfer and irradiation concept. Nucl. Instrum. Methods Phys. Res. Sect. A Accel. Spectrom. Detect. Assoc. Equip. 424 (1), 215–220. URL. http://www.sciencedirect.com/science/article/pii/S0168900298012510.

Grosse, M., Kuehne, G., Steinbrueck, M., Lehmann, E., Stuckert, J., Vontobel, P., Mar. 2008. Quantification of hydrogen uptake of steam-oxidized zirconium alloys by means of neutron radiography. J. Phys. Condens. Matter 20 (10), 104263. URL. http://iopscience.iop.org/0953-8984/20/10/104263.

Grosse, M., Steinbrck, M., Stuckert, J., Kastner, A., Schillinger, B., Sep. 2012. Application of neutron radiography to study material processes during hypothetical severe accidents in nuclear reactors. J. Mat. Sci. 47 (18), 6505–6512. URL. http://link.springer.com/article/10.1007/s10853-011-5553-1.

Grosse, M., Steinbrueck, M., Kaestner, A., Sep. 2011a. Wavelength dependent neutron transmission and radiography investigations of the high temperature behaviour of materials applied in nuclear fuel and control rod claddings. Nucl. Instrum. Methods Phys. Res. Sect. A Accel. Spectrom. Detect. Assoc. Equip. 651 (1), 315–319. URL. http://www.sciencedirect.com/science/article/pii/S0168900211005055.

Grosse, M., van den Berg, M., Goulet, C., Lehmann, E., Schillinger, B., Sep. 2011b. In-situ neutron radiography investigations of hydrogen diffusion and absorption in zirconium alloys. Nucl. Instrum. Methods Phys. Res. Sect. A Accel. Spectrom. Detect. Assoc. Equip. 651 (1), 253–257. URL. http://www.sciencedirect.com/science/article/pii/S0168900210028111.

Grosse, M.K., Stuckert, J., Steinbrck, M., Kaestner, A.P., Hartmann, S., 2013. Neutron radiography and tomography investigations of the secondary hydriding of Zircaloy-4 during simulated loss of coolant nuclear accidents. Phys. Procedia 43, 294–306. URL. http://www.sciencedirect.com/science/article/pii/S1875389213000497.

Hansche, B.D., 1989. Film-based computed tomography of nuclear-fuel-damage experiments. Mat. Eval. 47 (6), 741–745. URL. http://cat.inist.fr/?aModele=afficheN&cpsidt=7275566.

Hausladen, P.A., 2013. Demonstration of Emitted-neutron Computed Tomography to Count Fuel Pins. Tech. Rep. DE2013–1079266. Oak Ridge National Lab, USA. URL. http://info.ornl.gov/sites/publications/Files/Pub37069.pdf.

Hofmann, G., Berndt, R., Schone, M., Nagel, S., Sep. 1988. Nuclear-fuel tomography. Kernenergie 31 (9), 394–396 wOS: A1988Q764100005.

Holcombe, S., Jacobsson Svrd, S., Eitrheim, K., Hallstadius, L., Willman, C., Jul. 2013. Feasibility of identifying leaking fuel rods using gamma tomography. Ann. Nucl. Energy 57, 334–340. URL. http://www.sciencedirect.com/science/article/pii/S0306454913001011.

Honda, S., Ikeda, Y., Koike, M., Tomatsu, Y., Matsumoto, G., Fujine, S., 1990. Fine neutron CT with film method. In: Fujine, S., Kanda, K., Matsumoto, G., Barton, J. (Eds.), 3rd World Conf on Neutron Radiography. Kluwer Academic Publ, Osaka, Japan, pp. 827–834 wOS: A1990BS32Z00094.

Hsue, S.T., Crane, T.W., Talbert, W.L.J., Lee, J.C., Jan. 1978. Nondestructive Assay Methods for Irradiated Nuclear Fuels. Tech. Rep. LA-6923. Los Alamos Scientific Lab., N.Mex. (USA). URL. http://www.osti.gov/scitech/biblio/5153553.

IAEA, I., 2002. IAEA Safeguards Glossary. Tech. Rep. IAEA/NVS/3/CD. International Atomic Energy Agency, Vienna.

Ishimi, A., Katsuyama, K., Maeda, K., Nagamine, T., Asaga, T., Furuya, H., Dec. 2012. Upgrading of X-ray CT technology for analyses of irradiated FBR MOX fuel. J. Nucl. Sci. Technol. 49 (12), 1144–1155. URL. http://dx.doi.org/10.1080/00223131.2012.740354.

Jacobsson, S., Feb. 2000. A Tomographic Method for Verification of the Integrity of Spent Nuclear Fuel. Ph.D. thesis. Uppsala University, Uppsala, Sweden. URL: http://www.kth.se/polopoly_fs/1.469394!/A\%20Tomographic\%20Method\%20for\%20Verification\%20of\%20the\%20Integrity\%20of\%20Spent\%20Nuclear\%20Fuel.pdf.

Jacobsson, S., Bcklin, A., Hkansson, A., Jansson, P., Nov. 2000. A tomographic method for experimental verification of the integrity of spent nuclear fuel. Appl. Radiat. Isot. 53 (45), 681–689. URL. http://www.sciencedirect.com/science/article/pii/S0969804300002050.

Jacobsson Svaerd, S., Haakansson, A., Lundqvist Saleh, T., 2008. Verification of Completeness of Spent Nuclear Fuel Assemblies by Means of Tomography. URL. http://inis.iaea.org/Search/search.aspx?orig_q=RN:41116204.

Jansson, P., Jacobsson Svrd, S., Hkansson, A., Bcklin, A., 2006. A device for nondestructive experimental determination of the power distribution in a nuclear fuel assembly. Nucl. Sci. Eng. 152 (1), 76–86. URL. http://uu.diva-portal.org/smash/record.jsf?pid=diva2:164457.

Je, U.K., Lee, M.S., Cho, H.S., Hong, D.K., Park, Y.O., Park, C.K., Cho, H.M., Choi, S.I., Woo, T.H., Dec. 2014. Simulation and experimental studies of three-dimensional (3d) image reconstruction from insufficient sampling data based on compressed-sensing theory for potential applications to dental cone-beam CT. Nucl. Instrum. Methods Phys. Res. Sect. A Accel. Spectrom. Detect. Assoc. Equip. 784, 550–556. URL. http://www.sciencedirect.com/science/article/pii/S0168900214015393.

Jenssen, H.K., Oberlander, B.C., Beenhouwer, J.D., Sijbers, J., Verwerft, M., Apr. 2014. Neutron radiography and tomography applied to fuel degradation during ramp tests and loss of coolant accident tests in a research reactor. Prog. Nucl. Energy 72, 55–62. URL. http://www.sciencedirect.com/science/article/pii/S0149197013002151.

Jonkmans, G., Anghel, V.N.P., Jewett, C., Thompson, M., Mar. 2013. Nuclear waste imaging and spent fuel verification by muon tomography. Ann. Nucl. Energy 53, 267–273 arXiv: 1210.1858. URL. http://arxiv.org/abs/1210.1858.

Jonkmans, G., Anghel, V.N.P., Thompson, M., 2010. Muon Tomography for Imaging Nuclear Waste and Spent Fuel Verification. URL. http://inis.iaea.org/Search/search.aspx?orig_q=RN:44055325.

Katsuyama, K., Maeda, K., Nagamine, T., Furuya, H., Jan. 2010. Three-dimensional X-Ray CT image of an irradiated FBr fuel assembly. Nucl. Technol. 169 (1), 73–80 wOS:000272916200006.

Kim, J., 2010. X-Ray tomography based simulation feasibility analysis of nuclear fuel pellets. J. Korean Soc. for Nondestruct. Test. 30 (4), 324–329. URL. http://www.kci.go.kr/kciportal/ci/sereArticleSearch/ciSereArtiView.kci?sereArticleSearchBean.artiId=ART001471720&locale=en&SID=W17sdDrUCdShXc45tNA.

Kim, W.K., Lee, Y.W., Cho, M.S., Park, J.Y., Ra, S.W., Park, J.B., Dec. 2008. Nondestructive measurement of the coating thickness for simulated TRISO-coated fuel particles by using phase contrast X-ray radiography. Nucl. Eng. Des. 238 (12), 3285–3291. URL. http://www.sciencedirect.com/science/article/pii/S0029549308003051.

Kim, W.K., Lee, Y.W., Park, J.Y., Park, J.B., Rhee, Y., Ra, S.-W., 2006. Nondestructive measurement of the coating thickness in the simulated TRISO-coated fuel particle using micro-focus x-ray radiography. J. Korean Soc. for Nondestruct. Test. 26 (2), 69–76. URL. http://www.kci.go.kr/kciportal/ci/sereArticleSearch/ciSereArtiView.kci?sereArticleSearchBean.artiId=ART001007665&locale=en&SID=W17sdDrUCdShXc45tNA.

Kosarev, L.I., Kuzelev, N.R., Yumashev, V.M., 1987. Radiometric Computer Tomography: Experimental Study on Effectiveness of Application to Control of Fuel Elements of Nuclear Reactors. URL. http://inis.iaea.org/Search/search.aspx?orig_q=RN:21024204.

Kotiluoto, P., Wasastjerna, F., Kekki, T., Sipil, H., Banzuzi, K., Kinnunen, P., Heikinheimo, L., Aug. 2009. Emission and transmission tomography systems to be developed for the future needs of Jules Horowitz material testing reactor. Nucl. Instrum. Methods Phys. Res. Sect. A Accel. Spectrom. Detect. Assoc. Equip. 607 (1), 61–63. URL. http://www.sciencedirect.com/science/article/pii/S0168900209006032.

Kumar, U., Ramakrishna, G., Datta, S., Ravindran, V., 2000. Prototype gamma-ray computed tomographic imaging system for industrial applications. Insight Non-Destruct. Test. Cond. Monit. 42 (10), 662–666. URL. http://www.scopus.com/inward/record.url?eid=2-s2.0-0034300122&partnerID=40&md5=1970e4e54ba24636b467bc4869c0fbc6.

Kuzelev, N.R., Yumashev, V.M., 2001. New Opportunities of Joint Use of Radiation Introscopy and Computer Tomography for Non-destructive Testing. Slovenian Soc Nondestructive Testing, Fac Mech Engineering, Portoroz, Slovenia wOS:000176702600012.

Lechelle, J., Bleuet, P., Martin, P., Girard, E., Bruguier, F., Martinez, M., Somogyi, A., Simionovici, A., Ripert, M., Valdivieso, F., Goeuriot, P., Aug. 2004. Micro-XANES and X-ray microtomography study of oxidation state, morphology, and chemistry evolution during nuclear fuel sintering. IEEE Trans. Nucl. Sci. 51 (4), 1657–1661.

Lee, Y.-D., Block, R.C., Slovacek, R.E., Harris, D.R., Abdurrahman, N.M., Feb. 2001. Neutron tomographic fissile assay in spent fuel using the lead slowing down time spectrometer. Nucl. Instrum. Methods Phys. Res. Sect. A Accel. Spectrom. Detect. Assoc. Equip. 459 (12), 365–376. URL. http://www.sciencedirect.com/science/article/pii/S0168900200010160.

Lee, Y.-D., Chang, J.H., Lee, C.H., Kim, Y.-K., Nov. 2000. Simulation of spatial fuel assay using HANARO neutron beam. Appl. Radiat. and Isotopes 53 (45), 587–593. URL. http://www.sciencedirect.com/science/article/pii/S096980430000230X.

Lee, Y.-D., Na, W.W., Lee, Y.G., Yoon, W.K., Kwack, E.H., Oct. 1997. Sensitivity on the spatial assay for safeguards in the designed device. Appl. Radiat. and Isotopes 48 (1012), 1535–1541. URL. http://www.sciencedirect.com/science/article/pii/S096980439700153X.

Lehmann, E.H., Vontobel, P., Hermann, A., Dec. 2003. Non-destructive analysis of nuclear fuel by means of thermal and cold neutrons. Nucl. Instrum. Methods Phys. Res. Sect. A Accel. Spectrom. Detect. Assoc. Equip. 515 (3), 745–759. URL. http://www.sciencedirect.com/science/article/pii/S0168900203023568.

Lekeaka-Takunju, P., Khan, T., Bardel, C., Udpa, S., Udpa, L., Kim, J., Krzywosz, K., Aug. 2010. Assessment of nuclear fuel pellets using X-ray tomography. Int. J. Appl. Electromagn. Mech. 33 (3/4), 1267–1272. URL. http://search.ebscohost.com/login.aspx?direct=true&db=a9h&AN=54624199&site=ehost-live.

Lekeaka-Takunju, P., Khan, T., Harmon, G., Udpa, S., Udpa, L., Apr. 2011. X-ray tomographic inspection of nuclear fuel rods using a limited number of projections. Mat. Eval. 69 (4), 495–500 wOS:000289500300008.

Lekeaka-Takunju, P., Udpa, S., Udpa, L., Kim, J., Krzywosz, K., 2009. Simulation study on nuclear fuel pellets inspection based on X-Ray tomography. Tokyo 110. In: Chen, Z.M., Jiang, J., Ma, X. (Eds.), Applied Electromagnetics and Mechanics (Ii), Japan Society Applied Electromagnetics & Mechanics, vol. 13, pp. 405–406. wOS:000288880300204.

Levai, F., 1982. Computed tomographic methods for nuclear-fuel characterization and safeguard. Periodica Polytechnica-Electr. Eng. 26 (1–2), 153–169 wOS:A1982QX02700013.

Lim, J.S., 1990. Two-dimensional Signal and Image Processing. Prentice Hall, Englewood Cliffs, NJ, 710 pp.-1. URL. http://adsabs.harvard.edu/abs/1990ph...book.....l.

Lundqvist, T., Jacobsson Svrd, S., Hkansson, A., Oct. 2007. SPECT imaging as a tool to prevent proliferation of nuclear weapons. Nucl. Instrum. Methods Phys. Res. Sect. A Accel. Spectrom. Detect. Assoc. Equip. 580 (2), 843–847. URL. http://www.sciencedirect.com/science/article/pii/S0168900207012740.

Lundqvist, T., Jacobsson Svrd, S., Hkansson, A., Bcklin, A., Jun. 2010. Recent progress in the design of a tomographic device for measurements of the three-dimensional pin-power distribution in irradiated nuclear fuel assemblies. Nucl. Sci. and Eng. 165 (2), 232–239. URL. http://epubs.ans.org/?a=10321.

Mistry, R.K., Laxminarayana, B., Srivastava, R.K., 1996. 25 years of NDE in Fabrication of Zirconium Alloy Mill Products and Nuclear Fuel in the Nuclear Fuel Complex. URL. http://inis.iaea.org/Search/search.aspx?orig_q=RN:30025126.

Niculae, C., Craciunescu, T., Dobrin, R., 1996. On the reconstruction of the fisson products distribution in nuclear fuel rods. Int. J. of Energy Res. 20 (11), 999–1002. URL: http://onlinelibrary.wiley.com/doi/10.1002/(SICI)1099-114X(199611)20:11<999::AID-ER211>3.0.CO;2-N/abstract.

Oleinik, S.G., Boltenkov, V.A., Maslov, O.V., Mar. 2005. Passive Computer tomography of nuclear fuel. At. Energy 98 (3), 227–229. URL. http://link.springer.com/article/10.1007/s10512-005-0198-2.

Pan, L., Tsao, C., 1999. Performance of a modified two-dimensional gamma scan system in spent fuel pin studies. J. Nucl. Sci. Technol. 36 (11), 1089–1097. URL. http://www.scopus.com/inward/record.url?eid=2-s2.0-0033355943&partnerID=40&md5=f0bd32ccc61bd09d9a5df3454ef959ae.

Panakkal, J., Ghosh, J., Roy, P., 1986. Analysis of optical density data generated from neutron radiographs of uranium-plutonium mixed oxide fuel pellets inside sealed nuclear fuel pins. Nucl. Inst. Methods Phys. Res. B 14 (3), 310–313. URL. http://www.scopus.com/inward/record.url?eid=2-s2.0-0022676043&partnerID=40&md5=b6ab804a8840eb1a3d4c58907812e4e7.

Panakkal, J.P., 2013. Use of Penetrating Radiation Techniques for Nondestructive Evaluation of Nuclear Fuel Pins. Bhabha Atomic Research Centre, Department of atomic energy, Mumbai.

Panakkal, J.P., Ghosh, J.K., Roy, P.R., 1992. Nondestructive characterization of mixed oxide pellets in welded nuclear fuel pins by neutron radiography and gamma-autoradiography: nondestructive characterization of materials. In: Holler, P., Hauk, V., Dobmann, G., Ruud, C.O., Green, R.E. (Eds.), 3rd International Symposium, Saarbrucken (Germany), 36 Oct. 1988. Springer-Verlag, p. 832838 (1989). {NDT} & E International 25(45), 231 –. URL. http://www.sciencedirect.com/science/article/pii/096386959290240H.

Panakkal, J.P.D., Mukherjee, H.S.K., Oct. 2008. Nondestructive Evaluation of Uranium-plutonium Mixed Oxide (MOX) Fuel Elements by Gamma Autoradiography (Shanghai, China).

Parrat, D., Guimbal, P., Le Guillou, G., Simon, E., Boucher, L., 2013. The Future Underwater Neutron Imaging System of the Jules Horowitz MTR: an Equipment Improving the Scientific Quality of Irradiation Programs. URL. http://inis.iaea.org/Search/search.aspx?orig_q=RN:45103487.

Pleinert, H., Lehmann, E., Hammer, J., 1994. Review of neutron radiography applications at the swiss research reactor SAPHIR. Insight 36 (10), 807–809. URL. http://cat.inist.fr/?aModele=afficheN&cpsidt=4275477.

Porter, D., Tsai, H., 2012. Full-length U–x Pu–10zr (x = 0, 8, 19 wt.%) fast reactor fuel test in FFTF. J. of Nucl. Mat. 427 (1–3), 56–57.

Richards, W.J., McClellan, G.C., Tow, D.M., 1982. Neutron Tomography of Nuclear Fuel Bundles. URL. http://inis.iaea.org/Search/search.aspx?orig_q=RN:15018550.

Ross, A.M., 1977. Neutron Radiographic Inspection of Nuclear Fuels. URL. http://inis.iaea.org/Search/search.aspx?orig_q=RN:8343885.

Runkle, R.C., Chichester, D.L., Thompson, S.J., Jan. 2012. Rattling nucleons: new developments in active interrogation of special nuclear material. Nucl. Instrum. Methods Phys. Res. Sect. A Accel. Spectrom. Detect. Assoc. Equip. 663 (1), 75–95. URL. http://www.sciencedirect.com/science/article/pii/S016890021101847X.

Sah, D., Viswanathan, U., Ramadasan, E., Unnikrishnan, K., Anantharaman, S., 2008. Post irradiation examination of thermal reactor fuels. J. Nucl. Mat. 383 (1–2), 45–53.

Sanders, J.D., Lindsay, J.T., McGregor, D.S., 2002. Development of a GaAs-based neutron tomography system for the assay of nuclear fuel. In: Seibert, J.A. (Ed.), 2001 Ieee Nuclear Science Symposium, Conference Records, Vols. 1–4. Ieee, New York, pp. 2326–2329 wOS:000178495800509.

Sawicka, B.D., Murphy, R.V., Tosello, G., Reynolds, P.W., Romaniszyn, T., Dec. 1990. Computed tomography of radioactive objects and materials. Nucl. Instrum. Methods Phys. Res. Sect. A Accel. Spectrom. Detect. Assoc. Equip. 299 (13),

468–479. URL. http://www.sciencedirect.com/science/article/pii/0168900290908275.
Shea, T., Chitumbo, K., 1993. Safeguarding Sensitive Nuclear Materials: Reinforced Approaches. Tech. Rep. IAEA Bulletin, 3/, 1993, Vienna. URL. http://www.iaea.org/Publications/Magazines/Bulletin/Bull353/35301052327.pdf.
Sim, C.-M., Kim, T., Oh, H.S., Kim, J.C., Apr. 2013. Measurement of ballooning Gap size of irradiated fuels using neutron radiography transfer method and HV image filter. J. Korean Soc. Nondest. Test. 33 (2), 212–218. URL. http://koreascience.or.kr/article/ArticleFullRecord.jsp?cn=BPGGB1_2013_v33n2_212.
Skilling, J., Bryan, R.K., Nov. 1984. Maximum entropy image reconstruction: general algorithm. Mon. Not. Royal Astron. Soc. 211 (1), 111–124. URL. http://mnras.oxfordjournals.org/content/211/1/111.
Sotthivirat, S., Fessler, J.A., Mar. 2002. Image recovery using partitioned-separable paraboloidal surrogate coordinate ascent algorithms. IEEE Trans. Image Process. 11 (3), 306–317.
Steinbock, L., 1990. Tomography of nuclear fuel experiments with an electronic line scan camera. Nucl. Eng. and Des. 118 (1), 9–16. URL. http://www.scopus.com/inward/record.url?eid=2-s2.0-44949269497&partnerID=40&md5=7386fb1c49c2e15abe6c20ca8d73d2b1.
Steinbock, L., 1991. Transmission tomography of nuclear fuel pins and bundles with an electronic line camera system. J. Nucl. Mat. 178 (2–3), 277–283. URL. http://www.scopus.com/inward/record.url?eid=2-s2.0-0026104925&partnerID=40&md5=6c126d14307fc38a267aa73a29b87786.
Sugita, T., Bacon, J., Ban, Y., Borozdin, K., Izumi, M., Karino, Y., Kume, N., Miyadera, H., Mizokami, S., Morris, C.L., Nakayama, K., Otsuka, Y., Perry, J.O., Ramsey, J., Sano, Y., Yamada, D., Yoshida, N., Yoshioka, K., Aug. 2014. Cosmic-ray muon radiography of UO2 fuel assembly. J. Nucl. Sci. and Technol. 51 (7–8), 1024–1031. URL. http://dx.doi.org/10.1080/00223131.2014.919884.
Svalbe, I., van der Spek, D., Dec. 2001. Reconstruction of tomographic images using analog projections and the digital radon transform. Linear Algebra Appl. 339 (13), 125–145. URL. http://www.sciencedirect.com/science/article/pii/S0024379501004876.
Svard, S., Hakansson, A., Backlin, A., Osifo, O., Willman, C., Jansson, P., 2005. Nondestructive experimental determination of the pin-power distribution in nuclear fuel assemblies. Nucl. Technol. 151 (1), 70–76.
Svard, S.J., Hakansson, A., Backlin, A., Jansson, P., Osifo, O., Willman, C., 2006. Tomography for partial defect verification – experiences from measurements using different devices. ESARDA Bull. 33, 15–25.
Tamaki, M., Iida, K., Mori, N., Lehmann, E.H., Vontobel, P., Estermann, M., Apr. 2005. Dy-IP characterization and its application for experimental neutron radiography tests under realistic conditions. Nucl. Instrum. Methods Phys. Res. Sect. A Accel. Spectrom. Detect. Assoc. Equip. 542 (13), 320–323. URL. http://www.sciencedirect.com/science/article/pii/S0168900205002081.
Tanke, R.H.J., Jaspers, J.E., Gaalman, P.A.M., Killian, D., 1991. Applications of Tomography in Nuclear Research. URL. http://inis.iaea.org/Search/search.aspx?orig_q=RN:23008438.
Tisseur, D., Banchet, J., Duny, P.G., Vitali, M.P., Peix, G., Letang, J.M., 2007. Quality Control of High Temperature Reactors (HTR) Compacts via X-Ray Tomography. URL. http://inis.iaea.org/Search/search.aspx?orig_q=RN:39090638.
Tremsin, A.S., Vogel, S.C., Mocko, M., Bourke, M.A.M., Yuan, V., Nelson, R.O., Brown, D.W., Feller, W.B., Sep. 2013. Non-destructive studies of fuel pellets by neutron resonance absorption radiography and thermal neutron radiography. J. Nucl. Mat. 440 (13), 633–646. URL. http://www.sciencedirect.com/science/article/pii/S0022311513008283.
Tsupko-Sitnikov, M.V., Feb. 1991. RIT A new robust iterative technique for image reconstruction in emission tomography. J. Nucl. Mat. 178 (23), 274–276. URL. http://www.sciencedirect.com/science/article/pii/002231159190397P.
Vairalkar, M.J., Nimbhorkar, S.U., Jan. 2012. Edge detection of images using sobel operator. Int. J. Emerg. Technol. Adv. Eng. 2 (1), 291–293.
Wei, G., Han, S., Wang, H., Hao, L., Wu, M., He, L., Wang, Y., Liu, Y., Sun, K., Chen, D., 2013. Design of the testing set-up for a nuclear fuel rod by neutron radiography at CARR. Physics Procedia 43, 307–313. URL. http://www.sciencedirect.com/science/article/pii/S1875389213000503.
Yang, M., Li, R., Duan, J., Liang, L., Li, X., Liu, W., Meng, F., Dec. 2013a. Analysis of DR testing blind zone of spherical fuel elements for 10 MW high-temperature gas-cooled reactor. Ndt & E Int. 60, 77–86 wOS:000326005300009.
Yang, M., Liu, Q., Zhao, H., Li, Z., Liu, B., Li, X., Meng, F., Apr. 2014. Automatic X-ray inspection for escaped coated particles in spherical fuel elements of high temperature gas-cooled reactor. Energy 68, 385–398. URL. http://www.sciencedirect.com/science/article/pii/S0360544214002102.
Yang, M., Zhang, J., Song, S.-J., Li, X., Meng, F., Kang, T., Liu, W., Wei, D., Apr. 2013b. Imaging and measuring methods for coating layer thickness of TRISO-coated fuel particles with high accuracy. NDT & E Int. 55, 82–89. URL. http://www.sciencedirect.com/science/article/pii/S0963869513000261.
Yasuda, R., Matsubayashi, M., Nakata, M., Harada, K., Amano, H., Sasajima, F., Nishi, M., Horiguchi, Y., Feb. 2005. Application of neutron imaging plate and neutron CT methods on nuclear fuels and materials. IEEE Trans. Nucl. Sci. 52 (1), 313–316.